p21 (WAF1) is component of a positive feedback loop that maintains the p53 transcriptional program

Cell Cycle 10:6, 932-950; March 15, 2011; © 2011 Landes Bioscience

p21^{WAF1} is component of a positive feedback loop that maintains the p53 transcriptional program

Lisa Y. Pang,[1] Mary Scott,[1] Richard L. Hayward, Hisham Mohammed,[1] C. Bruce A. Whitelaw,[2] Graeme C.M. Smith[3] and Ted R. Hupp[1,*]

[1]CRUK Cell Signalling Unit; Institute of Genetics and Molecular Medicine; [2]The Roslin Institute and University of Edinburgh; Edinburgh, Scotland UK; [3]KUDos Pharmaceuticals; Cambridge, England UK

Key words: p53, mdm2, feedback, cancer, transcription

The regulation of p53 activity through the MDM2 negative feedback loop is driven in part by an extrinsic ATM-pulse that maintains p53 oscillations in response to DNA damage. We report here that the p53 pathway has evolved an intrinsic positive feedback loop that is maintained by the p53-inducible gene product p21^{WAF1}. p21-null cancer cells have defects in p53 protein turnover, reductions in MDM2-mediated degradation of p53, and reduced DNA damage-induced ubiquitination of p53. TLR3-IRF1 or ATM-dependent signaling to p53 is defective in p21-null cells and complementation of the p21 gene in p21-null cancer cells restores the p53 transcriptional response. The mechanism of p53 inactivity in p21-null cells is linked to a p53 protein equilibrium shift from chromatin into cytosolic fractions and complementation of the p21 gene into p21-null cells restores the nuclear localization of p53. A loss of p53 transcriptional function in murine B-cells heterozygous or homozygous null for p21 highlights a p21-gene dosage effect that maintains the full p53 transcriptional response. ATM inhibition results in nuclear exclusion of p53 highlighting a positive genetic interaction between ATM and p21. p21 protein oscillates in undamaged proliferating cells, and reductions of p21 protein using siRNA eliminate the DNA damage-induced p53 pulse. The p53 transcription program has evolved a negative feedback loop maintained by MDM2 that is counteracted by a positive feedback loop maintained by ATM-p21 the balance of which controls the specific activity of p53 as a transcription factor.

Introduction

The tumor suppressor protein p53 is a central component of a stress-activated signal transduction program that mediates a range of biological effects including DNA repair, apoptosis or senescence.[1] The distinct array of gene products induced by the p53 transcriptional response mediates its tumor suppressor functions.[2] Stress-specific upstream kinase signaling events control the p53 activation pattern; DNA damage induces an ATM-CHK2 signal; hypoxia induces a LKB-AMPK signal, oncogene activation induces the ARF-DAPK signaling cascades; and DNA virus infection can stimulate a CK1-dependent p53 activation suggesting together that different stresses recruit different signaling modules to activate p53.[3] Germline mutation or tumor derived mutation of these kinase networks can attenuate the p53 response and contribute to enhanced cancer incidence.[4]

The multiple upstream signaling pathways that activate p53 resulting in phosphorylation and proline isomerization converge upon the key positive co-factor of p53, the transcriptional co-activator and acetyltransferase p300, which promotes p53 acetylation.[5] Conversely, in undamaged cells signaling networks maintain the function of the key negative regulator of p53, the ubiquitin ligase MDM2.[6] Under these latter conditions, p53 protein is kept inactive by an undefined set of signaling pathways maintaining induction of its own inhibitor, MDM2.[7] This forms the basis for the MDM2-dependent negative feedback loop that keeps p53 activity in check.[8,9] More recent data has shown that WIP1 is a p53-inducible protein phosphatase that cooperates with MDM2 and forms a second key component of the p53-transcription-driven negative feedback loop.[10] Stresses that disengage the MDM2-negative feedback loop are ATM-dependent and results in signals that activate the p53 response.[11] Recent studies have also highlighted the existence of an extrinsically activated pulse that results in ATM-activating or MDM2/WIP1-inhibitory waves of p53 protein synthesis and degradation that have formed the basis for deeper understanding of feedback control of the p53 response.[12] Together, these biochemical and genetic studies form the evidence for the core paradigm around which the specific activity of p53 is maintained by a balance between positive co-factors like ATM and p53-inducible negative regulators MDM2 and WIP1.

Transgenic studies in mice have been central in solidifying key paradigms in the p53 response and mice offer the opportunity for quantitative genetics linked to cell signaling.[13] Deletion of p53 results in viable animals with a strikingly enhanced cancer incidence,[14] thus affirming that p53 is dispensable for development but essential in pathways that mediate cancer suppression. Further, the introduction of an additional or activated p53 allele

*Correspondence to: Ted R. Hupp; Email: ted.hupp@ed.ac.uk
Submitted: 12/03/10; Revised: 01/30/11; Accepted: 01/31/11
DOI: 10.4161/cc.10.6.15012

enhances tumor suppression,[15,16] sometimes at a specific stage in the carcinogenic process.[16] The p53 pathway can be subjected to quantitative analysis: deletion of one allele of p53 compromises damage-induced apoptosis to an intermediate degree compared to wt or null homozygous cells.[17] The introduction of an additional p53 allele or a hypomorphic MDM2 allele into transgenic animals produces enhanced tumor suppression.[18] The significant changes in p53 activity resulting from reduced or enhanced p53 gene dosage suggest that cells have not evolved a classic genetic dosage compensation mechanism built into the p53-MDM2 negative feedback loop. Thus, a deeper understanding of quantitative control of the p53-MDM2 feedback loop will likely advance our understanding of how the tumor suppressor function of p53 is controlled.

Theoretical modeling has given novel insight into biological control of the p53 pathway. Single cell analyses have shown that the relative amounts of MDM2 and p53 oscillate with a fixed amplitude and time interval.[19] The response of the p53-MDM2 axis to increased stress by increasing the number of oscillations was interpreted to mean that the p53-MDM2 feedback is digital. However, although negative feedback loops are required for oscillations to occur, a simple two component system incorporating MDM2 and p53 cannot oscillate.[20] In other words, an unresolved qualitative problem with the p53:MDM2 negative feedback loop model is that there is no molecular mechanism to explain how p53 activity is switched on in the first place in undamaged cells to induce MDM2-mediated degradation of the p53 protein. One resolution could come from mathematical modeling which suggested the possibility that there could be a positive input which has evolved an integration into the negative feedback loop.[21] Incorporating such a positive branch into the p53 negative feedback loop could resolve mathematical and biological discrepancies with the oscillating nature of the negative feedback loop.

A logical hypothesis could be made that one possible candidate for a positive transcriptional branch to the p53-MDM2 transcriptional feedback loop factor would be an intrinsic component; a p53-inducible gene product that counteracts MDM2 function. Such a candidate gene would form a positive feedback loop and it might also be a p53-inducible gene whose deletion in mice gives a similar phenotype to p53: enhanced cancer incidence. The p53-inducible gene p21 fulfils partially this criteria based on three key genetic studies; p21-null animals have an increased spontaneous cancer susceptibility, although are cancer prone at an older age than p53-null mice,[22] p21-null animals have an increase in metastatic tumors induced by irradiation,[23] and the tumor spectrum in ATM-p21 double null animals are similar to that observed in p53-null animals.[24] These latter data indicate that ATM and p21 are components of a positive genetic pathway that regulates cancer suppression in a manner similar to p53.

Given these tumor suppressor functions of p21 and the theoretical requirement of a positive component to the p53 feedback pathway, we evaluated the integrity of the p53 pathway in sets of cells with a reduced p21-gene dosage to determine whether p21 could be a component of a positive regulatory feedback. Our data demonstrate that loss of p21 compromises the p53 transcriptional response in part due to p53 protein mislocalization and that ATM-inhibition gives rise to a similar mislocalization of p53 protein. p53 appears to have evolved a co-ordinated transcription mechanism to control its own function via a positive branch maintained by p21 and a negative branch maintained by MDM2, the balance of which controls the specific activity of p53.

Results

Defects in p53 protein degradation and transcriptional activity in p21-null colorectal cancer cells. In order to begin to determine whether there is positive genetic interaction between the p53 pathway and the *p21* gene, we first evaluated p53 protein steady-state levels and protein half-life in isogenic wild-type (hereafter referred to as wt) and p21-null colorectal cancer cells.[25] There are higher steady state-levels of p53 protein in p21-null cells (**Fig. 1A**, lane 2 vs. 1) highlighting some perturbation in p53 protein homeostasis in the absence of p21 protein (**Fig. 1B**, lane 2 vs. 1). A similar change in p53 protein levels were reported previously in HCT116 p21-null cells, which was attributed to the ability of p21 to function as a negative regulator of p53 protein stability.[26] However, further analysis indicated that the elevated levels of wt-p53 protein in p21-null HCT116 cells is due to a striking increase in p53 protein half-life compared to p53 protein in wt-p21 containing cells (**Fig. 1E**, lane 1–5 vs. **Fig. 1G**, lane 1–5).

p53 protein can become more "stable" due to two distinct mechanisms; the first reflecting "activation" of the p53 transcriptional response by a signal and the second reflecting "inactivation" of p53 due to mutations that enhanced stability to do defects in MDM2-mediated degradation in p53-mutant cells. We performed experiments to distinguish between these two possibilities. The enhanced stability of p53 protein in p21-null cells was not attributed to a reduction in the specific activity of the proteasome (**Fig. 1I**). Rather, this enhanced stabilization of p53 protein and/or defects in p53 protein degradation in the p21-null cells is a classic signature of inactive, mutant p53 in cancer cells resulting from defects in induction of the MDM2-negative feedback loop.[27] Indeed, MDM2 protein induction is defective after ionizing radiation or doxorubicin treatment in p21-null HCT116 cells (**Fig. 1J and N** respectively, lanes 3 vs. 4), under conditions where p53 protein levels remain elevated (**Fig. 1L/K and O** respectively, lanes 3 and 4). As a control, a typical MDM2 protein induction after DNA-damage in wt-cells (**Fig. 1J and N**, lanes 2 vs. 1) can be compared to the standard p53 protein induction after DNA damage (**Fig. 1L/K and O**, lanes 1 vs. 2). Further, the classic ubiquitin-like modification on p53 protein induced by certain DNA damaging agents[28] such as ionizing radiation and doxorubicin (**Fig. 1L/K and O** respectively, lane 2 vs. 1) is also defective in the p21-null cells (**Fig. 1L/K and O**, lane 4 vs. 3), presumably due to attenuation in MDM2 protein induction. This stabilized p53 is transcriptionally inactive in p21-null cells as defined using a p53-responsive *p21 luc*-reporter based assays, relative to the p53-null HCT116 cell and the isogenic wt-HCT116 controls (**Fig. 1Q**). The data above indicate that p53 protein is highly stable, but transcriptionally attenuated, in p21-null colorectal cancer cells.

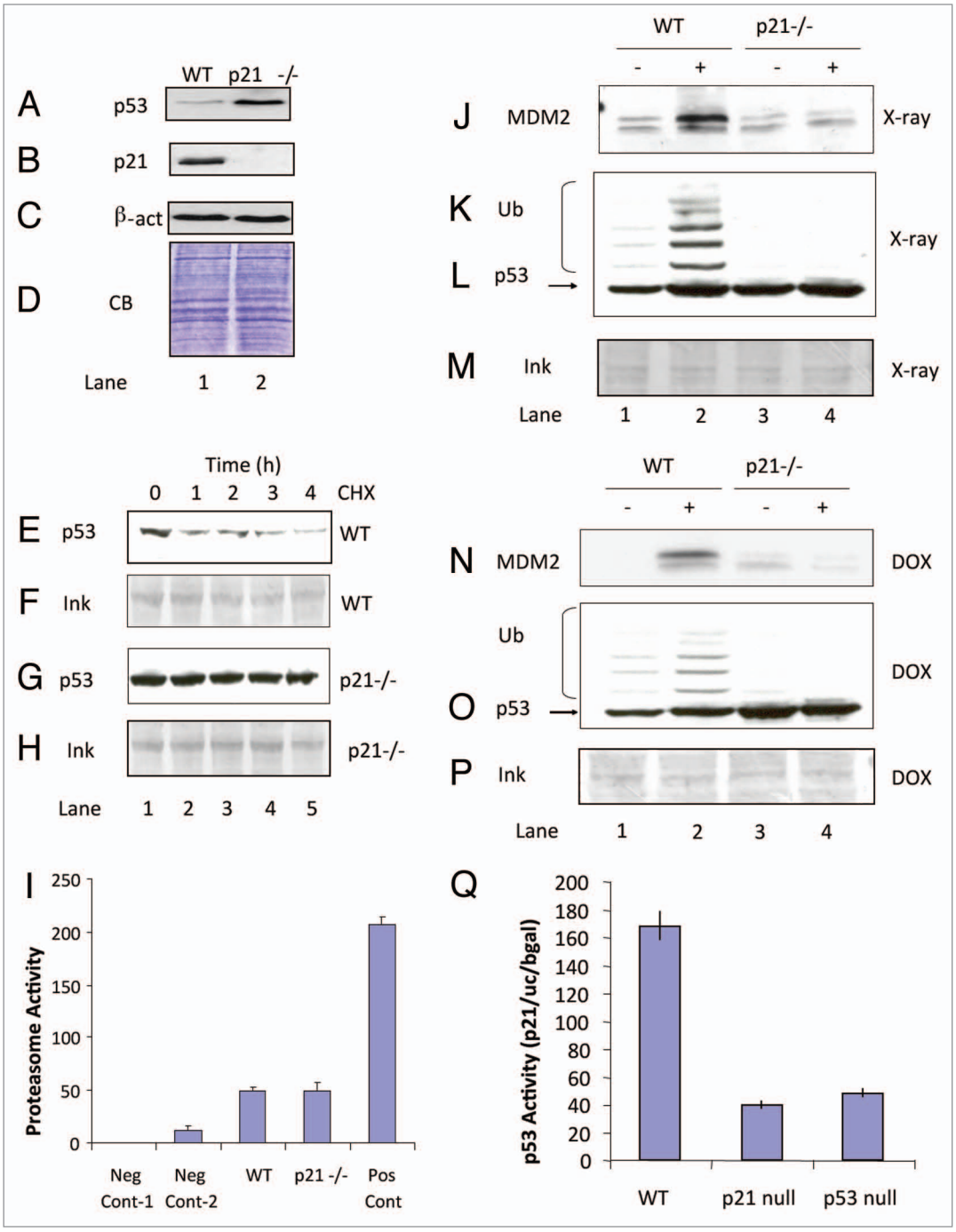

Figure 1. The p53 protein pathway is aberrant in p21-null cells. (A–D) Analysis of p53 protein steady-state levels in HCT116 wt and p21$^{-/-}$ cells. HCT116 WT and p21$^{-/-}$ cells were lysed in urea lysis buffer, whole cell lysates were resolved by SDS-PAGE, and the indicated proteins were detected by immunoblotting. (D) An additional loading control depicts Coommassie Blue dye staining of total protein. (E–H) High basal level of p53 in the p21$^{-/-}$ cells is due to increased half-life of p53. Lysates were prepared from HCT116 WT and p21$^{-/-}$ cells at 0–4 hr after addition of 30 μg/ml cyclohexamide (CHX) and p53 was detected by immunoblotting (E and G). Ink stain was used as a loading control (F and H). (I) Proteasome activity is unaffected in p21$^{-/-}$ cells. The 20s proteasome activity of HCT116 WT and p21$^{-/-}$ cells was determined by monitoring the release of a fluorophore AMC (7-amino-4-methylcoumarin) from a proteasome specific peptide, using a 20s Proteasome Assay Kit (Calbiochem). (J–P) MDM2 induction and damage induced Ubiquitination-like modifications on p53 is compromised in p21$^{-/-}$ cells. The indicated wt or p21$^{-/-}$ cell panels were treated with ionizing radiation (J–M) or doxorubicin (N–P) and the levels of MDM2 protein were analyzed by immunoblotting (J and N) and the levels of p53 protein (L and N) and ubiquitin-like adducts (K) were analyzed by Immunoblotting. Ink stain was used as a loading control (L and O). (Q) Specific reporter based transcriptional activity of p53 is reduced in p21$^{-/-}$ cells. The human p21 promoter fused to luciferase (1 μg) was introduced into HCT116 WT, p21$^{-/-}$ and p53$^{-/-}$ cells together with 1 μg pCMV-βgal reporter. Cells were harvested 24 hr after transfection and lysed with 5x Reporter Lysis Buffer (Promega). Luciferase activity was detected by a luminometer. p53-dependent activity (relative light units) is expressed as a ratio of p21-Luciferase activity to the internal transfection control β-gal.

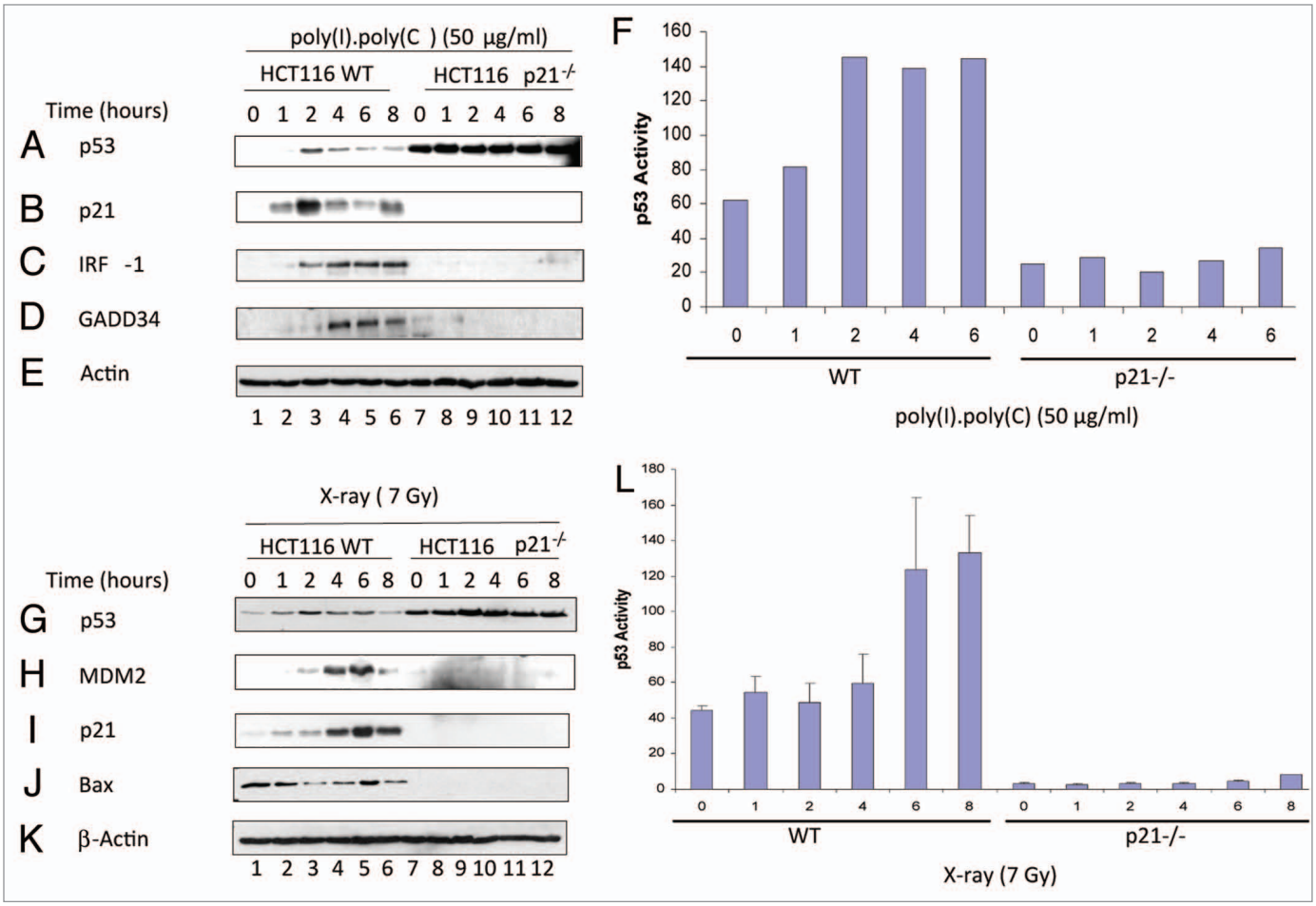

Figure 2. p53 pathway induction by poly(I).poly(C) or X-ray signaling is attenuated in p21-null cells. (A–E) The p53 TLR3 anti-viral response is suppressed in p21$^{-/-}$ cells. HCT116 WT and p21$^{-/-}$ cells were treated with the TLR3 ligand 50 μg/ml poly(I).poly(C) and harvested at the stated time points. Cells were lysed with urea lysis buffer. Whole cell lysates were resolved by SDS-PAGE and p53, p21, IRF-1 and GADD34 were detected by immunoblotting. β-actin was used a loading control. (F) p53 transcriptional reporter activity in response to poly(I).poly(C) was compromised in p21$^{-/-}$ cells. HCT116 WT and p21$^{-/-}$ cells were transiently transfected with 1 μg p21-Luciferase and 1 μg pCMV-βgal reporter and treated with 50 μg/ml poly(I).poly(C) 24 hr after transfection. Cells were harvested at the time points indicated and lysed with 5x Reporter Lysis Buffer (Promega). Luciferase activity was detected by a luminometer. p53-dependent activity (relative light units) is expressed as a ratio of p21-Luciferase activity to the internal transfection control β-gal. (G–K) The p53 ATM DNA damage response is suppressed in p21$^{-/-}$ cells. HCT116 WT and p21$^{-/-}$ cells were treated with 7 Gy of ionizing radiation (IR) and harvested at the stated time points. Cells were lysed with urea lysis buffer and whole cell lysates were resolved by SDS-PAGE and immunoblotting to detect p53, MDM2, p21, BAX and β-actin. (L) p53 transcriptional reporter activity in response to IR was compromised in p21$^{-/-}$ cells. HCT116 WT and p21$^{-/-}$ cells were transiently transfected with 1 μg p21-Luciferase and 1 μg pCMV-βgal reporter and treated with 7 Gy IR 24 hr post-transfection. Cells were harvested at the time points indicated and lysed with 5x Reporter Lysis Buffer (Promega). Luciferase activity was detected by a luminometer. p53-dependent activity (relative light units) is expressed as a ratio of p21-luciferase activity to the internal transfection control β-gal.

p53 responsive TLR3 and ATM signaling is defective in p21-null cells. To further evaluate whether there is a more profound defect in the stress-activated p53 transcriptional response in p21-null cells, selected endogenous p53-responsive protein and mRNA products were quantified after exposure of cells to two distinct physiologically relevant stresses resulting from anti-viral or DNA damage sensing pathways. p53 protein is known to be required for both DNA-damage and the DNA/RNA anti-viral response,[29] although how cells activate p53 in response to distinct stresses is not fully defined. Nevertheless, as p21-null cells are defective in p53 transcriptional activation in response to DNA damaging agents (**Fig. 1**), we evaluated whether the treatment of cells with the TLR3 ligand Polyinosinic polycytidylic acid [hereafter referred to as poly(I).poly(C)],[30] also resulted in reduced p53 activation in p21-null cells. If so, it would indicate a common signaling defect in both ATM-DNA damage (as in **Fig. 1**) and TLR3 signaling pathways. The treatment of wt-cells with poly(I).poly(C) results in the induction of p53 protein, IRF-1 protein stabilization, and GADD34 induction (**Fig. 2A–D**, lanes 2–6 vs. 1). By contrast, there was no detectable induction of IRF-1 or GADD34 proteins by poly(I).poly(C) in the p21-null cells (**Fig. 2C and D**, lanes 8–12 vs. 7). This was corroborated using the *p21luc* reporter where poly(I).poly(C) was only able to trigger *p21luc* reporter activity in the wt-p21 cells (**Fig. 2F**). As controls, a time course revealed the classic X-ray induced stabilization of p53 protein, MDM2 induction, and BAX perturbation after

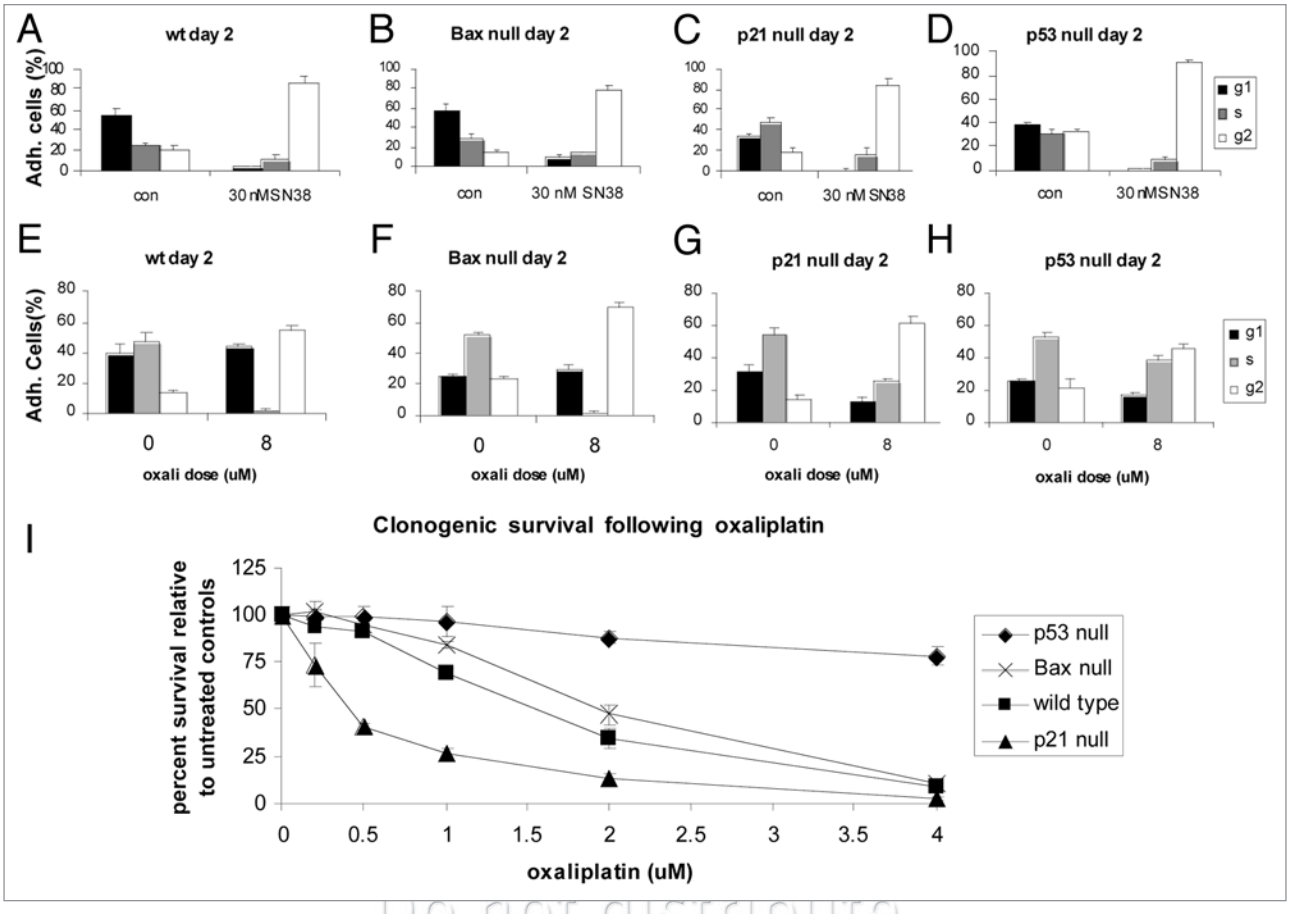

Figure 3. Cell cycle analysis of HCT116 wt and p21-null cells. The indicated HCT116 cell parts were treated as indicated (A–D) with SN38 and (E–H) with oxaliplatin. Cells were processed after (time) and processed for cell cycle analysis as reported previously in reference 32. (I) Clonogenic survival was also performed with the indicated cell parts as a function of oxaliplatin concentration.

irradiation in the wt-p21 cells (**Fig. 2G–J**, lanes 2–6 vs. 1). By contrast, MDM2 induction was not detected after irradiation nor was any BAX protein detected in the absence or presence of irradiation in the p21-null cells (**Fig. 2H and J**, lanes 8–12 vs. 7). This was corroborated using *p21luc* reporter assays where there were defects in the irradiation-induced activation of the p21 reporter (**Fig. 2L**).

As a control, we evaluated the integrity of the p21-null cells which have been previously shown to be sensitive to certain DNA damaging agents under conditions in which p53-null cells resist damage induced lethality.[25,31] Exposure of cells to the topoisomerase I inhibitor SN38[32] results in S-phase dependent DNA damage and a G_2/M arrest in a panel of HCT116 cells (wt, bax-null, p53-null and p21-null; **Fig. 3A–D**). These data indicate that the p21-null and wt cells exhibit an intact p53-independent checkpoint program in response to this insult. However, the exposure of wt or bax-null cells to oxaliplatin, which generates S-phase independent DNA damage, results in a G_1 cell cycle block (**Fig. 3E and F**) that is defective in p21-null and in p53-null cells (**Fig. 3G and H**). These data indicate that the p21-null and p53-null growth arrest phenotypes co-segregate and that the G_1 arrest damage response, which is at least in part dependent on p53 dependent transcription is selectively reduced in these genetic backgrounds. Clonogenic survival assays demonstrate that the p21-null cells are more sensitive to oxaliplatin under conditions where p53-null cells are more resistant, relative to wt-cells (**Fig. 3I**). Resistance of cells to certain damaging agents as a result of p53-deletion and conversely, the sensitivity as a result of p21-deletion has been observed previously in reference 33 and 34, indicating that the isogenic cell panels we used are representative. Thus, the apoptotic phenotypes of p21-null and p53-null cells do not co-segregate under these conditions, in contrast to the p53 dependent transcriptional phenotypes described above.

Complementation of the p21 gene in p21-null cells restores the p53 TLR3 and DNA damage response. The HCT116 cell line is hyper-recombination proficient and it remained possible that the p53 transcriptional defects seen in p21-null cells was due to additional mutations accumulated in these cells over time since their construction.[25] This might be less likely considering the survival and cell cycle parameters analyzed in **Figure 3** that recapitulate classic cell responses in the absence of p21. However, we evaluated whether reduced p53 activity in p21-null cells was a single gene defect by analyzing p53 function after the generation of p21-null clones which re-express the human p21 gene driven from a constitutive CMV promoter. Such p21-complemented cells re-express basal levels of BAX and MDM2 protein relative to p21-null cells which do not express detectable BAX or MDM2

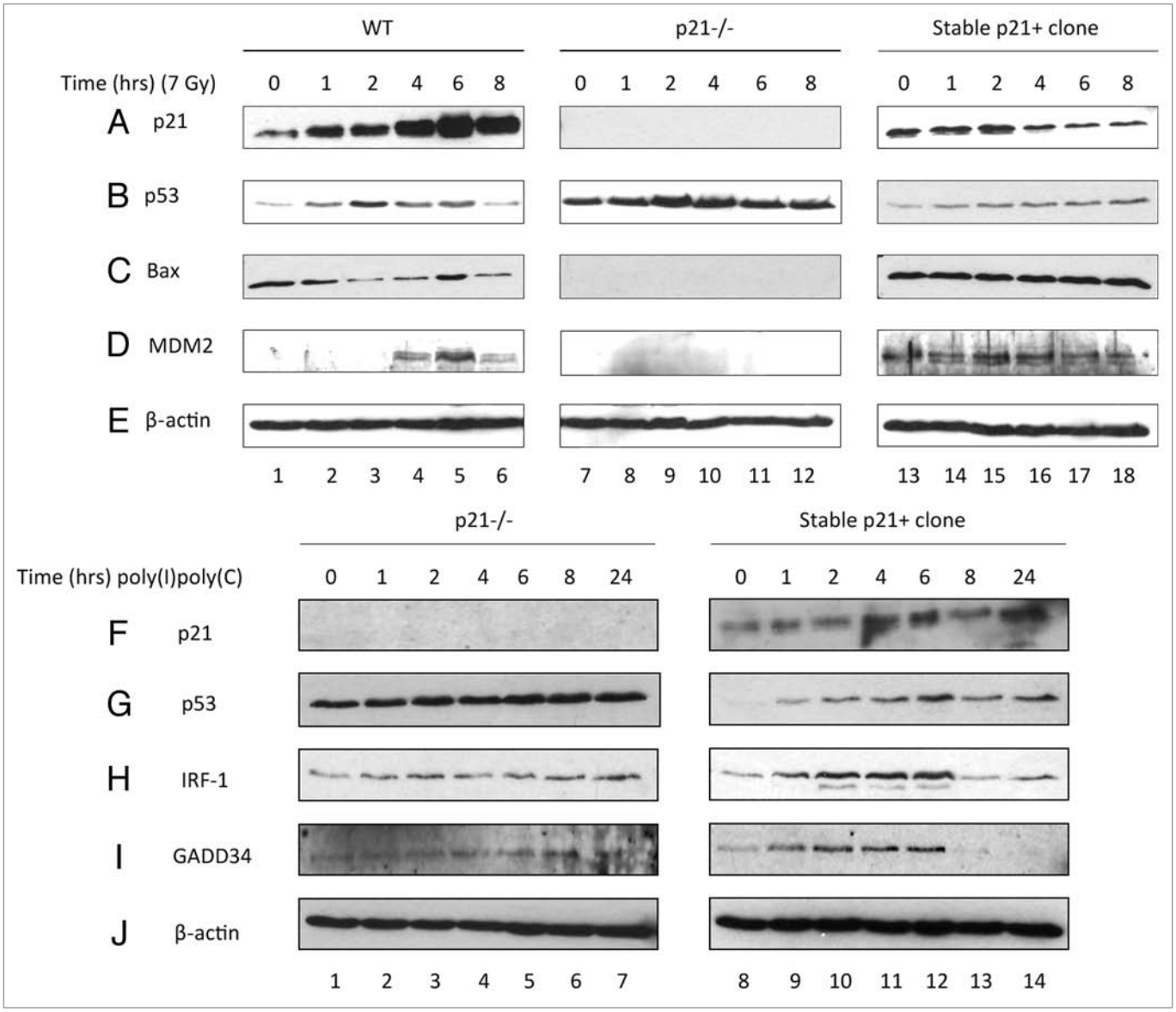

Figure 4. Complementation of the p21 gene into p21-null cells restores the p53 transcriptional response. HCT116 WT, p21$^{-/-}$, p21-complemented p21$^{-/-}$ cells were treated with the (A–E) IR or (F–J) poly(I).poly(C) and harvested at the stated time points. Cells were lysed with urea lysis buffer. Whole cell lysates were resolved by SDS-PAGE and the indicated proteins were quantified by immunoblotting.

proteins (**Fig. 4C and D**, lane 13 vs. lane 7). In response to DNA damage, the p21-complemeted cells also responded by transient induction of MDM2 protein (**Fig. 4D**, lanes 13–18). These data indicate that the classic p53 signature, namely MDM2 and BAX protein expression, can be restored in p21-null cells by complementation of the p21 gene. A similar reconstitution in TLR3 signaling was observed after complementing the p21 gene in p21-null cells. Relative to the control p21-null cells which fail to induce IRF1 or GADD34 after poly(I).poly(C) treatment (**Fig. 4H and I**, lanes 1–7), the p21 expressing p21-null cells exhibited poly(I).poly(C)-dependent induction of p53, IRF1 and GADD34 (**Fig. 4G–I**, lanes 8–14). These data indicate that the p53 transcription defect in p21-null cells is due predominately to a single gene defect.

Distinct subcellular localization of p53 protein in p21- null cells. As p53 protein is transcriptionally attenuated in response to two distinct stresses in the p21-null cell (**Fig. 2**), there is presumably a common mechanism that accounts for why different stress-responsive systems cannot engage the p53 pathway in this genetic background. Five of the most common ways for p53 protein to be inactivated include defects in ATM-pathway activation,[35] stimulation of MDM2-mediated trans-suppression of p53 at chromatin,[36] increases in histone deacetylase functions,[37] increases in p53 nuclear export,[38,39] and p53 protein unfolding and inactivation which can sensitize p53 to hyperubiquitination and degradation.[40,41] All of these phenomena have been shown to occur in cancer cell lines and provide an explanation for how the p53 protein pathway can be inactivated post-translationally in cancer cells.

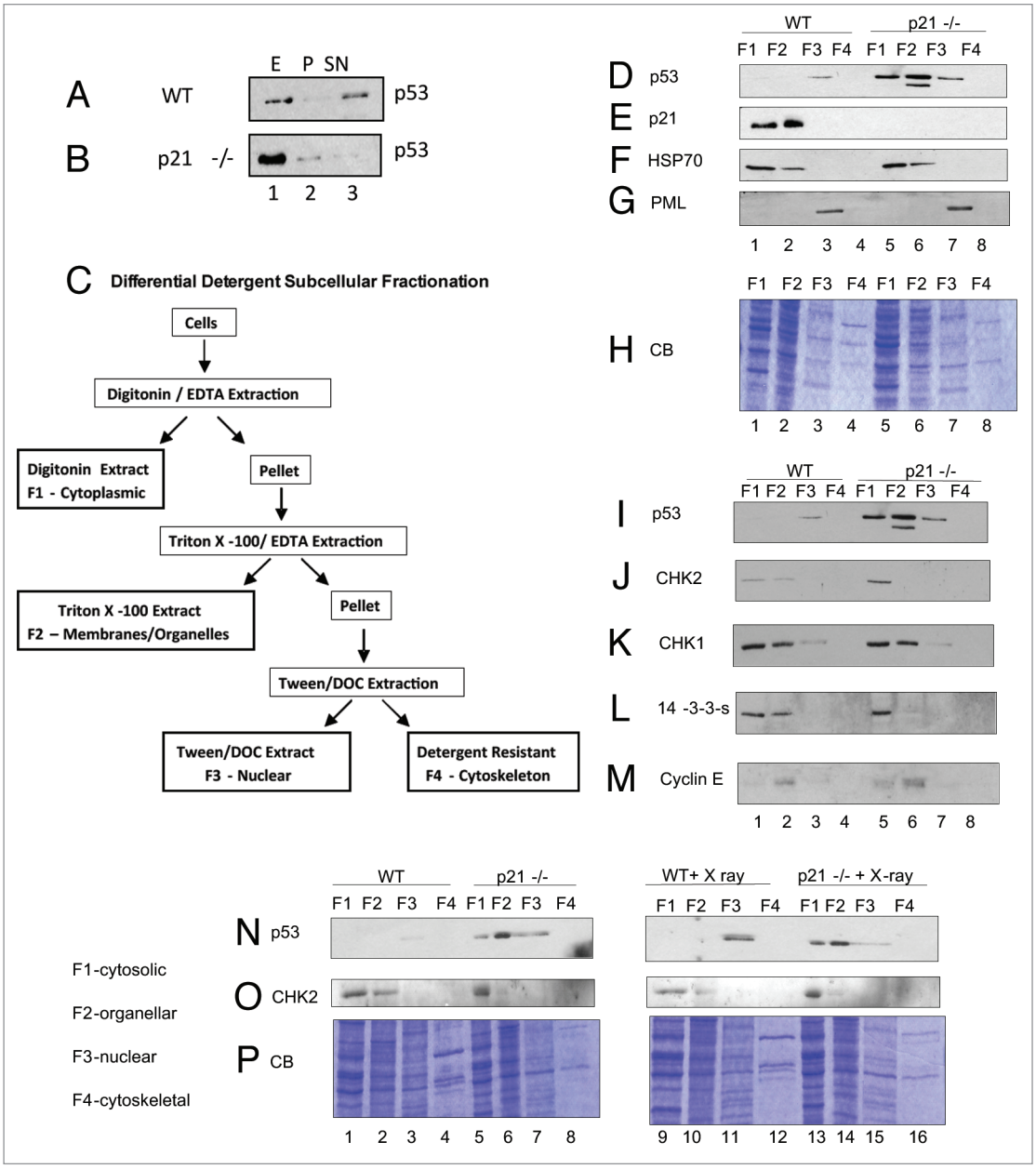

Figure 5. p53 protein is mislocalized in p21$^{-/-}$ cells. Loss of p21 is associated with mislocalization of p53 as defined using chemical sub-cellular fractionation. (A and B) p21$^{-/-}$ cells have reduced p53 protein in the chromatin fractions. Nuclei were isolated from HCT116 WT and p21$^{-/-}$ cells and were subsequently chemically fractionated into: E-total cellular extract; P-insoluble nuclear fraction; SN-soluble nuclear chromatin containing fractions as described previously in reference 42. p53 protein levels were detected by Immunoblotting. (C) Subcellular fractionation protocol. Proteins from HCT116 WT and p21$^{-/-}$ cells were extracted according to their subcellular localization: F1-Cytosol; F2-Membrane/organelle; F3-Nucleus; F4-Cytoskeleton (ProteoExtract® Subcellular Proteome Extraction Kit (S-PEK), Calbiochem®). (D–M) Selectivity of p53 mislocalization in p21$^{-/-}$ cells. The indicated cell lines were subjected to subcellular fractionation and the proteins from each fraction were resolved by SDS-PAGE and analyzed by immunoblotting for: p53; p21; HSP70, PML; CHK2; CHK1; 14-3-3; and Cyclin E. (N–P) p53 protein subcellular localization after irradiation. The indicated cell lines were subjected to subcellular fractionation before or after irradiation and the proteins from each fraction were resolved by SDS-PAGE and analyzed by immunoblotting for: p53, CHK2 and total protein after staining with Coommassie Blue.

We first evaluated whether p53 protein is in a "mutant" and inactive conformation in p21 null cells, which might occur if there were general misfolding defects. However, using monoclonal antibodies that can quantify the extent of folded or unfolded p53 protein, the p53 protein in wt and p21-null cells was in the wild-type conformation (data not shown). We next evaluated whether p53 protein has reduced association with chromatin fractions,[42] which might explain in part its lowered specific activity. On the other hand, if p53 protein was localized equivalently on chromatin fractions in wt and p21-null cells, there might be suppressing factors like MDM2 recruited to attenuate p53 function at promoters.[36] When nuclei are purified, chromatin is

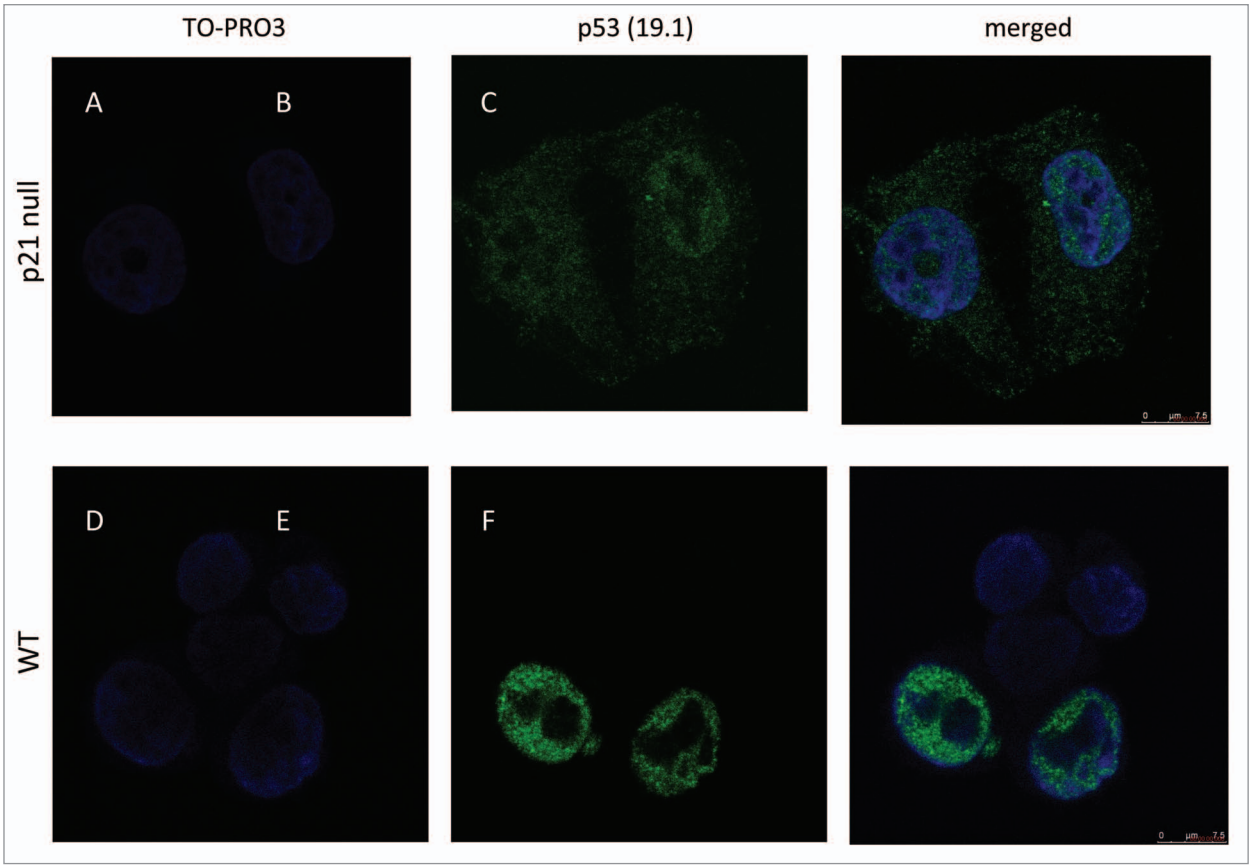

Figure 6. Enhanced cytoplasmic expression of p53 protein in p21-null cells defined using microscopy. The indicated cells [p21-null, (A–C); and wt-(D and E)] were fixed and processed for immunochemical evaluation of p53 protein localization with a TO-PRO3 nuclear counter stain using a Leica TCS SP5 confocal microscope.

extracted into the soluble nuclear fraction and remaining material sediments with insoluble material. In wt cells, the majority of p53 protein is present in the soluble chromatin fraction (**Fig. 5A**, lane 3) with little p53 present in the insoluble pellet (**Fig. 5A**, lane 2). However, in the p21-null cells, p53 protein is not chromatin associated but sediments in insoluble fractions (**Fig. 5B**, lane 2). These data indicate that in nuclear fractions from p21-null cells, the p53 is mislocalized away from soluble chromatin fractions and we therefore evaluated whether p53 protein is generally mislocalized in p21-null cells using chemical fractionation methodologies that can extract proteins differentially from distinct subcellular compartments (**Fig. 5C**).

Fractionation of cells into cytosolic, membrane, nuclear and cytoskeletal fractions demonstrated that p53 protein is predominantly nuclear in wt HCT116 colon cancer cells (**Fig. 5D**, lane 3), whereas p53 protein was largely cytosolic in the p21-null cells (**Fig. 5D**, lane 5 and 6). This change in localization is consistent with the distinct redistribution of p53 from the chromatin fractions in wt-cells to the insoluble nuclear pellet in p21-null cells (in **Fig. 5A and B**). This effect was relatively specific for p53, since HSP70 and PML were not grossly mislocalized in p21-null cells (**Fig. 5F and G**). Total protein content in each sub-cellular fraction can be evaluated qualitatively, as shown in **Figure 5H**. For comparison, other checkpoint proteins were also examined for changes in localization equilibrium including CHK2, CHK1, 14-3-3 and Cyclin E (**Fig. 5I–M**). As a control, DNA damage by irradiation of wt-cells increased the levels of p53 protein in the F3 nuclear fraction (**Fig. 5N**, lane 11 vs. 3), whereas irradiation of p21-null cells did not result in p53 nuclear accumulation (**Fig. 5N**, lane 13 and 14 vs. 5 and 6). Confocal microscopy was also used to reveal a shift of human p53 protein from predominantly nuclear pools in wt cells (**Fig. 6E**) to enhanced cytosolic pools in p21-null cells (**Fig. 6B**).

Complementation of the p21 gene into p21-null cells can restore the p53 pathway (**Fig. 4**) and we evaluated whether this correlated with nuclear re-localization of the p53 protein. Relative to the control samples in which p53 protein from wt-cells was distributed in the F3 nuclear fraction (**Fig. 7A**, lane 3) and p53 protein from p21-null cells was distributed in the cytosolic fractions (**Fig. 7A**, lane 5–7), the p21-null cells complemented with the p21 gene restored the F3 nuclear localization of p53 (**Fig. 7A**, lane 11). Further, p21 localized to the F1 and F2 cytosolic fractions in the complemented p21-null cells (**Fig. 7C**, lanes 9 and 10) that is similar to p21 subcellular localization in the wt-cells (**Fig. 7C**, lanes 1 and 2). The C-terminus of the p21 gene has the major binding site for PCNA, which comprises a major function of p21 (**Fig. 7E**).[43] A form of p21 with a deletion of the C-terminus (1-133) was able to stimulate

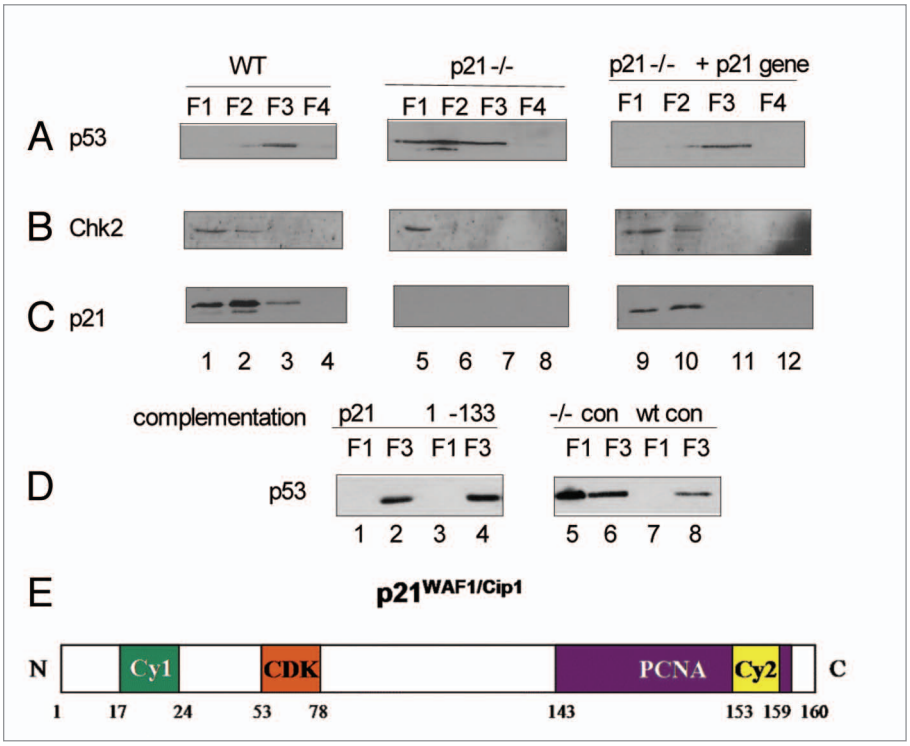

Figure 7. Complementation of the p21 gene into p21-null cells restores the p53 nuclear localization. (A–C) p53 localization in HCT116 cell parts. HCT116 WT, p21$^{-/-}$, p21-complemented p21$^{-/-}$ cells were subjected to subcellular fractionation and the proteins from each fraction were resolved by SDS-PAGE and analyzed by immunoblotting for: p53, CHK2 and p21. (D) p53 localization in HCT116 cell parts after p21 (1–133) complementation. p21$^{-/-}$ cells were transfected with full length p21 (lanes 1 and 2) or p21(1–133) (lanes 3 and 4) were subjected to subcellular fractionation and the proteins from each fraction were resolved by SDS-PAGE and analyzed by immunoblotting for p53. Controls fractionations included vector transfected p21$^{-/-}$ cells (lanes 5 and 6) and untransfected wt-cells (lanes 7 and 8). (E) Diagram of the p21 linear binding motif structure including the cyc1 and cyc2 helices, the cdk binding site, and the C-terminal PCNA binding site which is deleted in the truncated p21 (1–133) isoform.

the re-localization of p53 protein into the F3 nuclear fraction (**Fig. 7D**, lane 4 vs. 5 and 6) indicating that this p53 stimulatory function of p21 appears to be distinct from its PCNA binding functions. An uncoupling of p21 growth arrest functions from PCNA binding has been previously reported in reference 44.

Non-transformed cells require p21 to maintain maximal p53 function and nuclear localization. The experiments described thus far have examined the contribution of p21 to p53 function using a well-established colorectal cancer cell line. It remains possible that this function of p21 is confined to tumor cell lines and to evaluate this we evaluated the role of p21 in the p53 pathway in normal human fibroblasts. The reduction in p21 protein using siRNA to p21 (**Fig. 8A**, lane 2 vs. 1) results in reduced levels of the p53-responsive gene product BAX (**Fig. 8C**, lanes 2 vs. 1). This is suggestive of reduced p53 function and is similar to the reduced basal BAX protein in p21-null HCT116 cells (**Fig. 2**). A p53 gene expression array was used to evaluate whether there were defects in the expression of common p53-responsive genes after p21 protein depletion using siRNA. Relative to the control panels that produce the highlighted levels of p53 responsive genes (**Fig. 8E**), reduction in p21 resulted in substantial reduction in p53 responsive genes relative to controls (**Fig. 8F and H**). Irradiation can induce some of the p53-responsive genes in cells depleted of p21 protein (**Fig. 8G**), including CDK4 and MDM2 (**Fig. 8I and J**), indicating that siRNA depletion of p21 is not able to fully inactivate the p53 pathway. Subcellular fractionation studies also indicated that siRNA to p21 shifted the equilibrium of p53 from nuclear (**Fig. 8K**, lane 3) to the cytosolic fractions (**Fig. 8K**, lane 5). The elevated pool of nuclear p53 protein in cells depleted of p21 protein (and the increased activity after DNA damage) using siRNA might reflect the relative inefficiency of siRNA to fully deplete p21 protein, as is done by genetic deletion in the HCT116 cells.

A more quantitative genetic screen is therefore required to establish whether p21 plays a positive role in regulating the p53 transcriptional response in normal untransformed cells. Murine B-cells have proven to be a genetically well-defined in vitro cell model with which to analyze the pro-apoptotic function of p53 in vitro, for example reduced p53-dependent function after mutation of the transactivation domain phospho-acceptor site at Ser-23.[45] There have been previous reports indicating that animals have enhanced cancer susceptibility in a p21-heterozygote or p21-null background,[46] p21-null animals are tumor prone but tumors development is much more delayed than in p53-null animals,[22] p21-deletion attenuates the tumor suppressor function of super-p53 mice,[47] and p21 loss blocks senescence and stimulates tumorigenesis in renal but not intestinal tissue.[48] There is therefore precedence in p21-null murine cells for enhanced cancer phenotypes that could be consistent with reduced specific activity of p53. After purifying B-cells from: (1) wt p21 homozygous animals; (2) mice heterozygous for p21; and (3) animals null for the p21 locus, RNA was isolated to measure steady-state expression of known murine p53 responsive genes normalized to standardized control promoters. A quantitative reduction in p53-responsive gene levels were observed as a function of reduced p21 gene dosage (**Fig. 9A–C** and quantified in **F and G**). Some gene products like MDM2 are more sensitive to loss of one p21 allele (**Fig. 9H**), whilst other genes like BAX exhibit relatively higher activity in p21-heterozygotes and require both p21 alleles to be deleted before reduction in gene expression can be observed (**Fig. 9J**). The reductions in gene expression in the p21-null B cells can be attributed in part to the shift in p53 equilibrium from the nuclear F3 fraction to the cytosolic fractions (**Fig. 9D**, lanes 1 and 3 vs. lanes 5 and 7). Together, these studies indicate that normal human fibroblasts or murine B-cells require p21 to maximize the

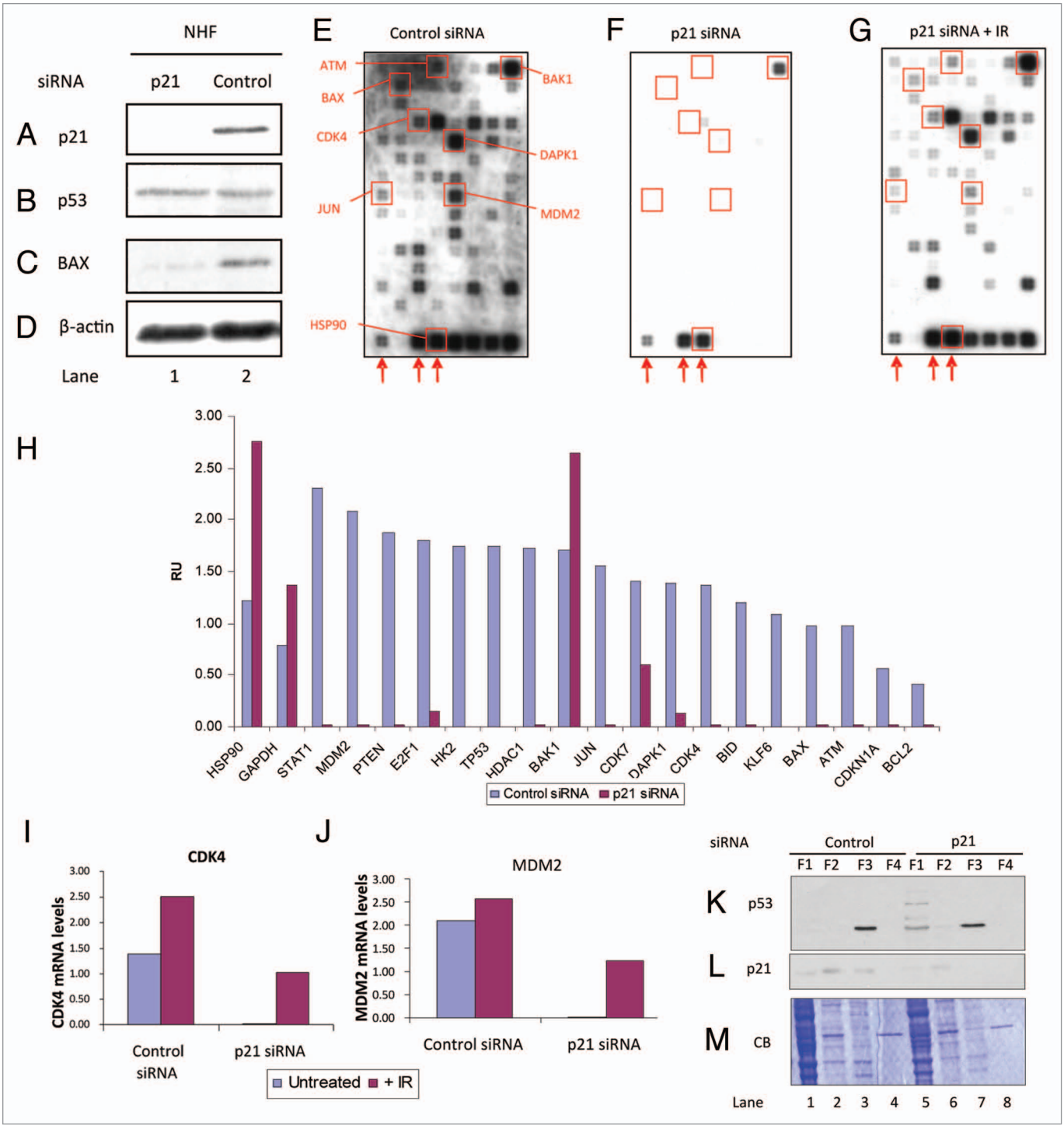

Figure 8. The p53 transcriptional response is attenuated by depleting p21 using siRNA in normal human fibroblasts. (A–D) p21 depletion using siRNA. Fibroblasts were treated with p21-specific or control siRNA for 48 hours and lysates were immunoblotted as indicated for p21, p53, Bax and β-actin. (E–H) p21 depletion using siRNA in normal human fibroblasts shows defects in basal and x-irradiation induced p53-dependent gene expression. Fibroblasts treated with control siRNA or p21-specific siRNA were left unirradiated (E and F) or irradiated with 7 Gy after p21-siRNA treatment (G) and incubated for 4 hr. DNA microarrays were used to profile the expression of genes related to p53-mediated signal transduction (OligoGEArray® System, SuperArray) to indicate the extent of p53 activity. Housekeeping gene expression is indicated by red arrows. The part of genes analyzed in detail are indicated by the red boxes and representative changes in gene expression of selected p53 responsive genes using GEArray Expression Analysis Suite software. (H) Graphical representation of NHF microarray results shows a general reduction of gene expression in the absence of p21. Gene expression is partially recovered in response to x-irradiation. Representative genes include CDK4 (I) and MDM2 (J). (K–M) p53 protein is mislocalized in normal human fibroblasts treated with siRNA specific for p21. Fibroblasts treated with control or p21-specific siRNA were extracted according to their subcellular localization: F1-Cytosol; F2-Membrane/organelle; F3-Nucleus; F4-Cytoskeleton (ProteoExtract® Subcellular Proteome Extraction Kit (S-PEK), Calbiochem®). Proteins from each fraction were resolved by SDS-PAGE and analyzed by immunoblotting for: p53, p21 and total Coommassie blue stained protein.

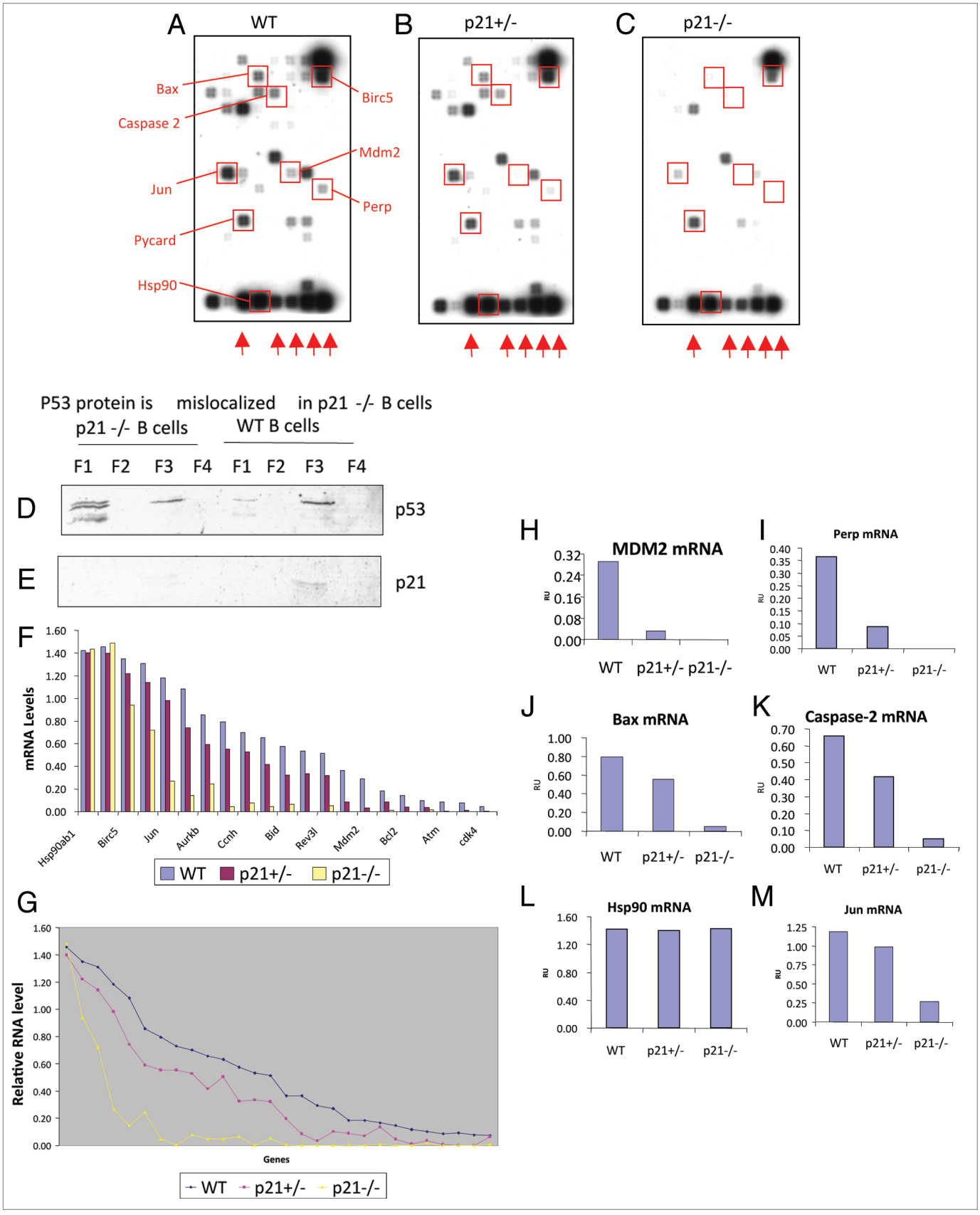

Figure 9. For figure legend, see page 943.

nuclear localization and transcriptional activity of p53 protein and that the p53 response is quantitatively responsive to p21 gene dosage.

p53 protein equilibrium shift from the nuclear to cytosolic fractions induced by ATM inhibition. The mechanism of how p21 maintains nuclear p53 and primes the transcription response is currently undefined. Two predominating ways for wt-p53 protein to be inactivated in cancers include defects in ATM-pathway activation and stimulation of MDM2-mediated nuclear export, transrepression, and/or degradation of p53 protein. p53 protein is not de-stabilized by p21 gene deletion; indeed there are defects in MDM2-dependent p53 degradation in the absence of p21 (**Fig. 1**). However, the apparent exclusion of p53 protein from chromatin fractions in the absence of p21 might indicate an activated MDM2 export pathway despite their being very low levels of MDM2. However, the treatment of p21-null cells with the MDM2-inhibitor Nutlin[49] does not completely restore nuclear localization of p53 protein in p21-null cells (**Fig. 10A**, lanes 13–15 vs. lane 9–11), under conditions where treatment of wt-cells with Nutlin resulted in enhanced p53 protein predominantly in the F3 nuclear fraction (**Fig. 10A**, lane 7 vs. 3). Under these conditions, Nutlin reduces the levels of MDM2 in the nuclear F3 fraction (**Fig. 10C**, lane 3 vs. 7) and increases MDM2 in the F1 cytosolic fraction (**Fig. 10C**, lane 1 vs. 5). These data indicate that low levels of MDM2 activity per se cannot account for the redistribution of p53 from chromatin to cytosolic fractions in p21-null cells.

If p21 is a component of an intrinsic positive feedback loop, then it is likely that the protein interacts with the extrinsic ATM-dependent p53 activating system. A recent report has highlighted that ATM is a component of an extrinsic DNA damage recognition system that maintains waves of p53 protein stabilization and degradation after DNA damage.[12] Further, ATM and p21 deletion cooperate to promote a tumor spectrum similar to p53-null animals.[24] It could be predicted that the mechanism of p21-mediated activation of the p53 pathway therefore involves p21-dependent control over ATM. As such, we examined whether ATM inhibition induces the phenotype observed in p21-null cells; equilibrium shift involving p53 nuclear exclusion and accumulation of cytosolic p53 protein. The treatment of HCT116 cancer cells with the specific ATM inhibitor (KU55993,[50]) resulted in significant cytosolic accumulation of p53 protein (**Fig. 10D**, lanes 5 and 6 vs. 1 and 2) that was similar to the redistribution of p53 protein observed in p21-null cells (**Fig. 10D**, lanes 9 and 10). As a control, the treatment of wt HCT116 cells with a specific DNA-PK inhibitor did not alter p53 protein nuclear localization (**Fig. 10F**, lanes 7 vs. 3). This effect of ATM-inhibition on redistribution of p53 protein from the nucleus to cytosolic fractions was also observed in normal human fibroblasts (**Fig. 10L**, lane 5 vs. 1), under conditions in which the DNA-PK inhibitor had no effect on p53 localization (**Fig. 10L**, lanes 9 and 11 vs. lanes 1 and 3). Finally, the redistribution of p53 protein from the nuclear to the cytosolic fraction after siRNA to p21 in normal human cells (**Fig. 10H**, lanes 5 and 6 vs. 1 and 2) was not rescued after depletion of MDM2 using siRNA (**Fig. 10K**, lanes 5 and 6 vs. **Fig. 10I**, lanes 5 and 6). These data indicate that the predominant mechanism of p21-maintenance of p53 protein localization is ATM-dependent and not MDM2-dependent.

p21 protein oscillates and maintains the ATM-p53 pulse after DNA damage. ATM is a component of an extrinsic DNA damage recognition pathway that maintains p53 protein activation pulses.[12] Accordingly, given that p53 nuclear localization in undamaged cells depends on both p21 and ATM gene products (**Fig. 10**) we evaluated whether p21 protein is a component of a similarly cycling system. In growing HCT116 cells, p21 protein exhibits an oscillating pattern (**Fig. 11A** and p21 part, lanes 2, 7, 12 and 18) giving a periodicity of approximately 2.5–3 hours. This oscillation of p21 is generally uncoupled from basal MDM2 protein levels over the 10 hours time course (**Fig. 11A** and MDM2 part). In MCF7 cells which are classically used to study p53 activation and which were used to originally define the ATM pulse,[12] undamaged cells also exhibit a cycling p21 protein expression pattern (**Fig. 11D and E**, lanes 1–9) with a periodicity of approximately 4 hours. Under these conditions, p53 and MDM2 proteins gradually accumulated as cells reached more confluent conditions (**Fig. 11B/C and F/G**, lanes 1–9), but neither p53 nor MDM2 exhibited the same degree of oscillation as p21 protein. After ionizing irradiation (2.5 Gy), the progressively decaying pulse of p53 is induced (**Fig. 11B and C**, lanes 13, 15 and 18), along with a consistently elevated p21 oscillation (**Fig. 11D and E**, lanes 15 and 18), and an MDM2 pulse (**Fig. 11F and G**, lanes 13, 15 and 18). The irradiation-induced p53, MDM2, and p21 pulse are largely co-incident after 2.5 Gy irradiation (lanes 13, 15 and 18). At higher doses of radiation (5 Gy), the p53 pulse is not evident (**Fig. 11**, lanes 19–26); presumably the p53 pulse is sensitive to the extent of damage and higher levels of irradiation might reflect a less physiologically relevant extent of DNA damage.

Together, these data indicate that p21 and ATM form a positive genetic interaction that cooperates to maintain p53 protein activity. p21 is the most sensitive factor to oscillations under steady-state proliferating conditions (**Fig. 11**) and plays a role in the maintaining the p53 pulse after DNA damage since siRNA targeted to attenuate p21 protein abrogates the p53 pulse at

Figure 9 (See opposite page). Analysis of p53-dependent gene expression alterations in $p21^{+/+}$, $p21^{+/-}$ and $p21^{-/-}$ murine B cells. (A–C) murine p53-gene array. B cells isolated from animals with the following genotype ($p21^{+/+}$, $p21^{+/-}$ and $p21^{-/-}$) were processed for total RNA isolation. DNA microarrays were used to profile the expression of genes related to p53-mediated signal transduction (OligoGEArray® System, SuperArray) to indicate the extent of p53 activity in the indicated genetic backgrounds. Normalization of housekeeping gene expression are indicated by red arrows. The part of genes analyzed in detail are indicated by the red boxes and representative changes in gene expression as a function of genetic background of selected p53 responsive genes using GEArray Expression Analysis Suite software (F and G; http://www.sabiosciences.com/support_software.php) are highlighted in parts (H–M) and include MDM2, Perp, Bax, Caspase-2, Hsp90 and Jun. (D and E) p53 protein is mislocalized in $p21^{-/-}$ B cells. Protein from B-cells were extracted according to their subcellular localization: F1-Cytosol; F2-Membrane/organelle; F3-Nucleus; F4-Cytoskeleton (ProteoExtract® Subcellular Proteome Extraction Kit (S-PEK), Calbiochem®). Proteins from each fraction were resolved by SDS-PAGE and analyzed by immunoblotting for p53 and p21.

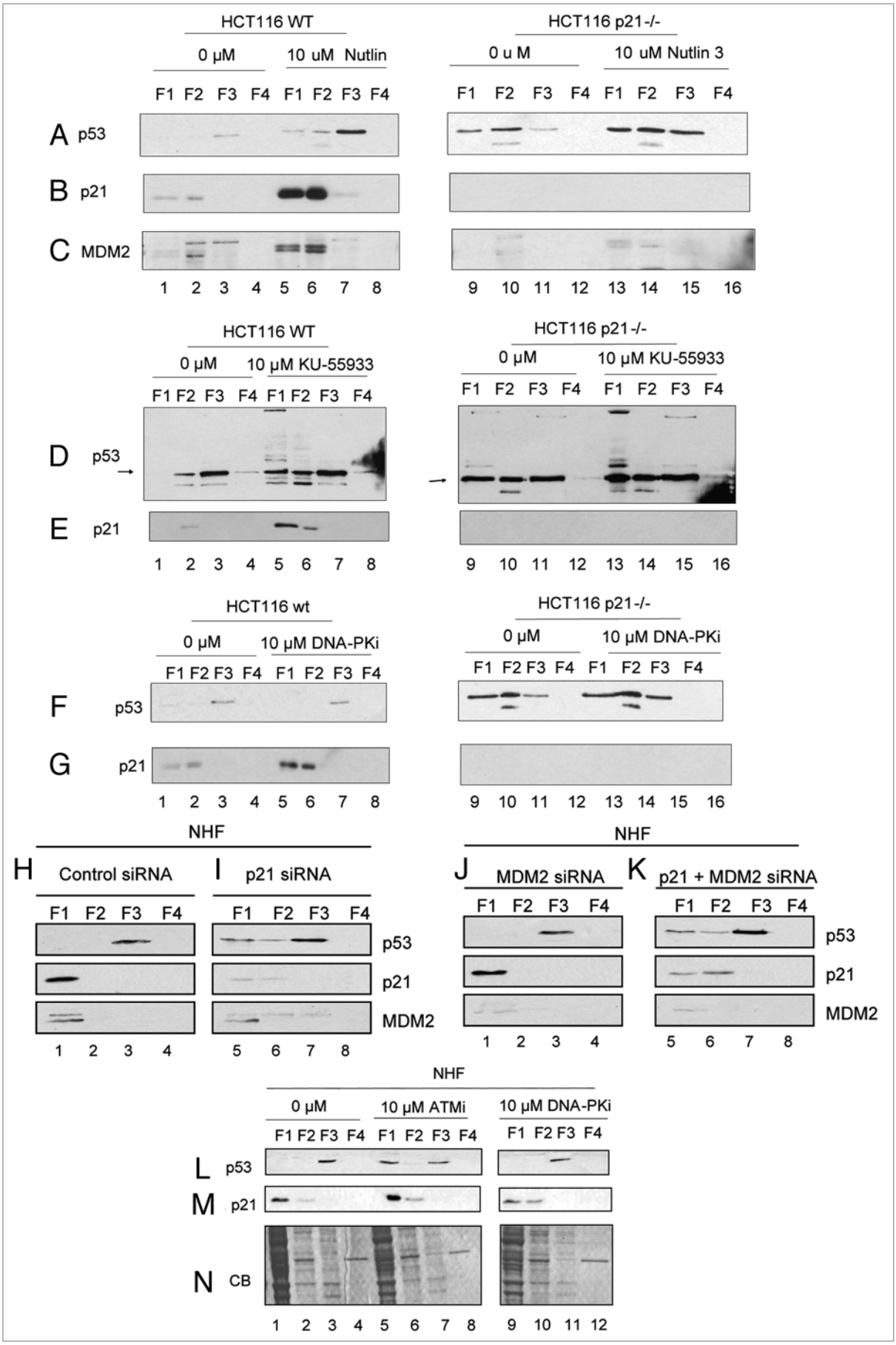
HCT116 WT
0 μM
10 uM Nutlin
HCT116 p21-/-
0 u M
10 uM Nutlin 3
F1 F2 F3 F4 F1 F2 F3 F4
A p53
B p21
C MDM2
1 2 3 4 5 6 7 8
9 10 11 12 13 14 15 16
HCT116 WT
0 μM
10 μM KU-55933
HCT116 p21-/-
0 μM
10 μM KU-55933
D p53
E p21
HCT116 wt
0 μM
10 μM DNA-PKi
HCT116 p21-/-
0 μM
10 μM DNA-PKi
F p53
G p21
NHF
H Control siRNA
I p21 siRNA
J MDM2 siRNA
K p21 + MDM2 siRNA
p53
p21
MDM2
NHF
0 μM
10 μM ATMi
10 μM DNA-PKi
L p53
M p21
N CB

2.5 Gy of radiation (**Fig. 11I**, lanes 1–10). This latter point is important, as it is not p53 protein stabilization by damage that is necessarily defective upon transient inhibition of ATM with a chemical inhibitor or attenuation of p21 using siRNA, but it is the pulses that are compromised in the absence of ATM or p21. These data suggest again that p21 plays a role in maintaining ATM activity, which is consistent with the fact that the ATM inhibitor induces the same p53 nuclear exclusion phenotype as p21-null cells (**Fig. 10**). Accordingly, we evaluated whether there were defects in ATM-phosphorylation after DNA damage in p21-null cells. After irradiation of wt-cell, a classic induction of ATM phosphorylation is observed at 1–2 hours post radiation (**Fig. 11J**, lane 2 and 3). However, in the p21-null cells, this full activation of ATM is delayed until 6 hours post irradiation (**Fig. 11J**, lanes 10) highlighting a quantitative defect in ATM activation in p21-null cells. Together, these data suggest that p21 forms a component of an intrinsic positive feedback loop that interacts with the extrinsic ATM pathway maintaining p53 protein in a transcriptionally competent state.

Discussion

The p21 gene as a genetic modifier of p53-dependent transcription. The p53 transcription program involves hundreds of genes whose functions are linked to many aspects of biology including anti-viral responses, metabolic stress, aging and genetic instability.[51] Of these many p53-induced genes, there are now two (MDM2 and WIP1) that are part of a negative feedback loop that functions to maintain low levels of p53 activity in undamaged cells but which are now known to play a role in the extrinsic ATM-"p53-pulse" induced by DNA damage.[12] The complete number of components to the p53 negative feedback loop are currently undefined. Feedback loops are integral components in biochemical and genetic signaling pathways that maintain stability in the biological network and the p53-MDM2 feedback appears to operate like a digital system.[19] However, one of the striking features of the p53 response to DNA damage is that there is no dosage compensation in $p53^{+/-}$ heterozygote cells[14,52] and p53 "knock-ins" have elevated p53 signaling responses;[15] i.e., if the MDM2-feedback loop operated with a strict dosage compensation mechanism then $p53^{+/-}$ and $p53^{+/+/+}$ animals would have cells with the same p53 specific activity. The fact that p53 activation appears rate-limiting, rather than p53 inhibition, suggests that the negative feedback loop is not rate-limiting and that MDM2 does not drive p53 into a steady-state equilibrium that is independent of p53-gene dosage. Mathematical modeling has provided novel insight into this problem; a positive and negative signal appears to operate in the p53 feedback loop and experiments were proposed on methodologies to tackle these paradigms.[21] The incorporation of a positive feedback loop to the p53 feedback pathway would provide a mechanism to account for lack of dosage compensation and would also suggest that the positive branch would be rate-limiting.

We reasoned that a positive branch integrated into the p53 negative feedback loop could be an intrinsic factor (i.e., a gene induced by p53) rather than an extrinsic factor (i.e., like ATM-DNA damage response[12]). As such, we first examined whether one of the first genes identified as a p53-inducible gene product, $p21^{WAF1}$, might be a component of a positive feedback. p21 was originally identified and characterized molecularly as a novel p53-induced gene product that could mediate a cell cycle arrest by virtue of blocking cyclin-dependent protein kinase function.[53,54] Although proposed originally to be a "mediator" of p53 tumor suppressor functions,[53] this concept was not so well supported based on the earlier data showing that p21-null animals do not have the same cancer incidence as p53-null animals.[46] However, it is now known that $p21^{+/-}$ animals have elevated tumor cell proliferation relative to $p21^{+/+}$,[46] and p21-null animals are more tumor prone though not at the younger age of p53-null animals.[22] Our data demonstrate that loss or of attenuation of p21 can stimulate nuclear export of p53, inhibition of p53 function, and enhanced stabilization of transcriptionally inactive p53. As such, p21 can fulfil the definition of a factor that can function in a positive feedback loop towards p53 protein that is counteracted by negative feedback loop factors like MDM2 (**Fig. 11K**). This is consistent with earlier discoveries that high levels of p53 protein caused by transcriptional inhibitors can be functionally attenuated with reduced responsiveness to stresses such as DNA damaging agents.[55,56] These data together indicate that factors that mediate degradation of p21 protein would attenuate p53 function and perhaps stabilize the p53 protein in a non-functional state by virtue of reducing the MDM2-dependent negative feedback loop. Such factors that regulate p21 protein stability include protein kinases like atypical-PKCs and ubiquitin ligases like MDM2 or proteasomal subunits that in turn could regulate p53 protein function.[57-60]

Other genetic studies have supported a role for p21 as a tumor modifier. One striking alteration of *p21* knockout keratinocytes is their very aggressive tumorigenic behavior after *ras* oncogene transformation.[61] Although p21 is thought to be one of the primary mediators of p53-induced growth inhibition, its role in p53 tumor suppression has been questioned, as p21 knockout mice do not exhibit an increased rate of spontaneous tumor formation relative to p53-null mice.[62] However, the spontaneous tumors formed in the p53 knockouts do not involve the epidermis, suggesting that p53 may exert different

Figure 10 (See opposite page). Effects of ATM and MDM2 inhibition using small molecules on p53 subcellular localization. (A–C) Nutlin effects on p53 localization. The indicated cell parts (wt or $p21^{-/-}$) were treated with Nutlin as indicated. (D–G) PI3K effects on p53 localization in HCT116 cell parts. The indicated cell parts (wt or $p21^{-/-}$) were treated with the indicated inhibitors (ATM (KU55993) or DNA-PK). Protein was extracted according to their subcellular localization: F1-Cytosol; F2-Membrane/organelle; F3-Nucleus; F4-Cytoskeleton (ProteoExtract® Subcellular Proteome Extraction Kit (S-PEK), Calbiochem®). Proteins from each fraction were resolved by SDS-PAGE and analyzed by immunoblotting for p53, MDM2, p21. (H–N) Effects of ATM inhibitors in normal human fibroblasts. Fibroblasts were treated, as indicated with siRNA targeting p21 and MDM2 or with the kinase inhibitors specific for ATM or DNA-PK.

tumor suppressing functions in this tissue. In fact, mutation and/or loss of the p53 gene has been shown to play an important role in chemically induced mouse skin carcinogenesis, but only in the late stages of benign to malignant tumor conversion.[16] The possibility that p53 and p21 genes have at least partially overlapping tumor suppressing functions in keratinocytes is indicated by the highly aggressive tumorigenic behavior of *ras* transformed p21 knockout keratinocytes, which is similar to that previously reported for *ras*-transformed keratinocytes with a p53 deletion.[63] A recent study has also supported an involvement of the p21 gene in p53-mediated tumor suppression.[47] In a $p21^{+/+}$ and p21-null background, p53-dependent pathways (apoptosis, cell cycle block and cancer incidence) were quantified by examining tumor susceptibility in mice carrying two or three copies of the p53 gene. The loss of p21 reduced the normally enhanced p53-mediated cell cycle arrest in the triploid-p53 background and also reduced the cancer suppressor function of the super-p53 mice in fibrosarcomas. These data suggest that the p53-dependent cell cycle arrest driven through the p21 gene plays an important role in mediating p53-dependent cancer protection and is consistent with the positive role for p21 in maintaining the transcription program in our current studies. However, the HCT116 p21-null cells remain sensitive to damage induced apoptosis (**Fig. 3**) and the p53-apoptotic program is maintained in the p21-null super-p53 mice[47] suggesting that the p53-p21 positive feedback loop might confined genetically to the growth arrest or possible transcription-dependent senescence pathway. Alternatively, the p53 protein that accumulates cytosolically in p21-null cells might function as a pro-apoptotic signal via mitochondrial-dependent and p53 transcriptional-independent pro-apoptotic pathways.[64]

The observations in this report that ATM inhibition or p21 attenuation promotes p53 cytosolic accumulation suggest a positive genetic interaction between the two proteins in maintaining a transcriptionally active p53 protein. This is consistent with the phenotypes observed in the ATM and p21 double-null mice. The tumor spectrum observed in these latter animals mice can be divided into two groups. The first group are those whose early tumor spectrum was lymphomas and sarcomas, which was similar to that observed in p53-null mice.[24] The second group are those whose late-onset cancers are not frequently observed in mouse models of cancer except in a telomerase deficient animal model and p53 mutant knock-in mouse models for Li-Fraumeni syndrome.[65] The development of carcinomas in the ATM and

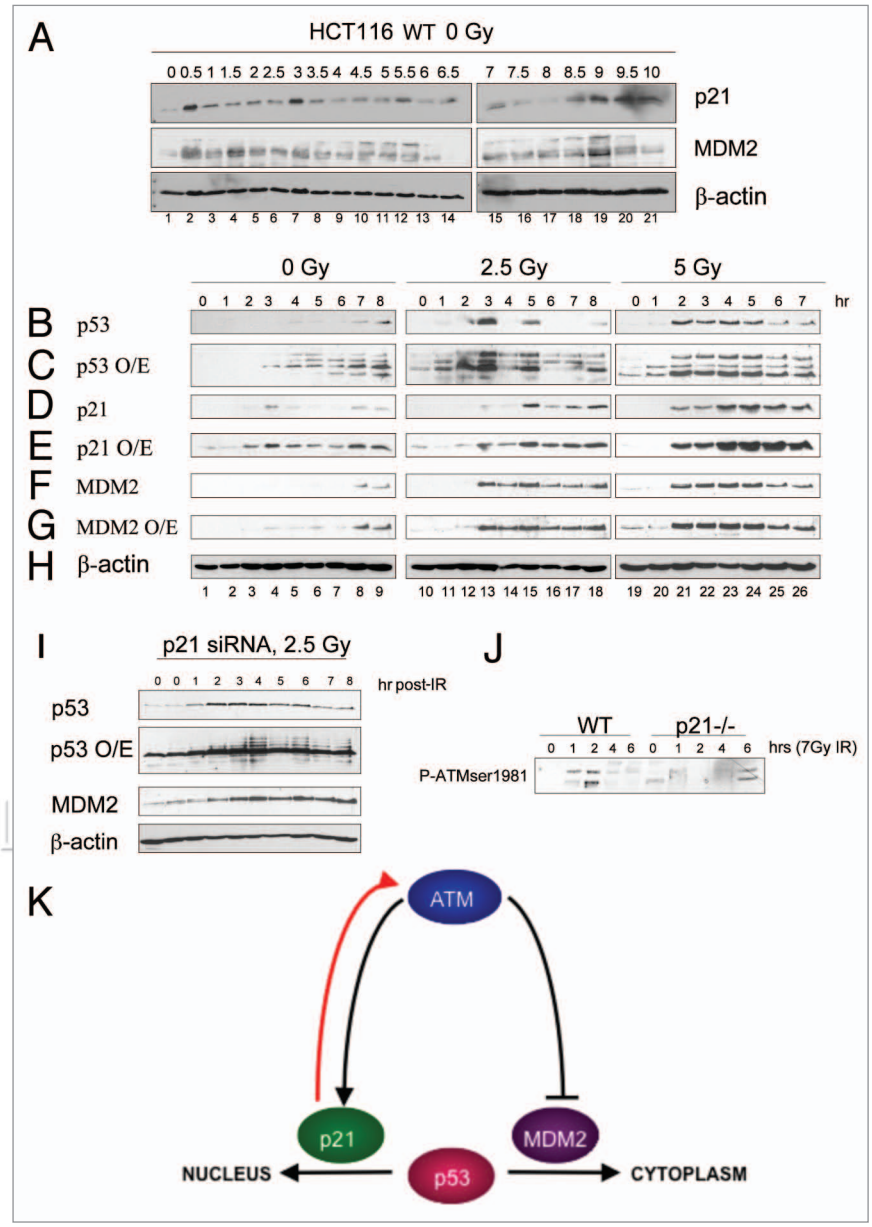

Figure 11. The role of p21 in regulating X-ray induced p53 protein oscillation. (A) p21 oscillations in cycling cells. HCT116 cells were plated at very low density and cells were harvested every half hour for the indicated time course for immunoblotting p21, MDM2 and actin. (B–H) Analysis of the dynamic changes p53-p21-MDM2 levels after irradiation. MCF7 cells were left untreated (lanes 1–9) or irradiated with 2.5 Gy or 5 Gy of ionizing radiation (lanes 10–26). Lysates were immunoblotted to detect p53, p21 and MDM2 protein levels. (O/E) indicates and over-exposure of the chemiluminescent detection to observe low levels of the indicated proteins. (I) Effects of p21 siRNA on the p53 pulse. MCF7 cells were irradiated after p21 depletion using siRNA and the effects of radiation on the p53 pulse was evaluated by immunoblotting for MDM2 and p53. (J) Defects in ATM activation in $p21^{-/-}$ cells. The indicated cell parts were exposed to ionizing radiation and immunoblotted for phospho-ATM at the indicated times points post-damage. (K) Model highlighting the relationship between two p53-inducible gene products-MDM2 and p21-one of which is a negative regulator and catalyzes p53 degradation by the proteasome and the other is an intrinsic positive effector and maintains nuclear localization of p53 plus the extrinsic ATM DNA damage pulse.

p21 double-null mice is of particular interest in its epistatic correlation with TERT and p53 double null mice since ATM activates p53 in response to DNA damage and is also involved in telomere maintenance. Our current studies involve understanding further how compartmentalization of the "intrinsic" (i.e., p53-depenent genes) p53 pathway composed of positive effectors like p21 or negative effectors like MDM2-WIP1 function to regulate the intrinsic p21 oscillation and the extrinsic ATM-p53-pulse that is activated by DNA-damage.[12]

Materials and Methods

Experimental reagents. Primary antibodies against β-actin, GADD34, HSP70, PML, 14-3-3σ and Cyclin E were purchased from Abcam (Cambridge, UK). Anti-IRF-1 antibody was purchased from BD Biosciences (Oxford, UK). Primary antibodies against MDM2 (4B2), and p53 (DO1) were obtained from Moravian Biotechnology (Brno, Czech Republic). Anti-p21 (Ab1) antibody was purchased from Calbiochem (Nottingham, UK). Primary antibodies against Bax (N-20), CHK1 (G-4) and CHK2 (A-12) were purchased from Santa Cruz (CA USA).

Cell culture and isolation of mouse B-cells. The HCT116 $p21^{-/-}$, $p53^{-/-}$ and $Bax^{-/-}$ isogenic derivatives of the wild-type HCT116 (HCT116 WT) colorectal cancer cell line, generated by targeted homologous recombination, were a generous gift from B. Vogelstein (John Hopkins Oncology Center, Baltimore, MD). Cells were maintained in McCoy's 5A medium. Normal human Fibroblast (NHF) cells were obtained from Promocell (Heidelberg, Germany) and maintained in HepesBSS medium. MCF-7 cells were maintained in Dulbecco's modified Eagles medium. All media was supplemented with 10% fetal bovine serum (Invitrogen Inc., Carlsbad, CA) and cells were maintained at 37°C in a humidified 5% CO_2 incubator. p21 homozygous (*Cdkn1a*$^{-/-}$) heterozygous (*Cdkn1a*$^{+/-}$) and wild type (*Cdkn1a*$^{+/+}$) mice were supplied by the Roslin Institute, Midlothian UK. The homozygous mice mating system was purchased from The Jackson Laboratory (Maine), JAX® Mice strain name: B6; 129S2-*Cdkn1a*^{tm1Tyj}/J. The isolation of B cells from mice spleens was achieved using the QuadroMACS™ separation system (Miltenyi Biotec, Bergisch Gladbach, Germany). Spleens were removed from mice and stored at 4°C in IMDM media supplemented with 5% Fetal bovine serum and 50 μM 2-mercaptoethanol. Each spleen was macerated with a fine syringe needle and cells were flushed out. Generally, ~1 x 10^8 cells per spleen were obtained. Cells were centrifuged at 300 *g* for 10 min at 4°C. The cell pellet was resuspended in 900 μl separation buffer (2 mM EDTA, 0.5% BSA in PBS pH 7.2) and 100 μl CD45R mouse MACS® Microbeads (Miltenyi Biotec, Bergisch Gladbach, Germany), and incubated for 15 min at 4°C. Cells were washed with 10 ml separation buffer and resuspended in 500 μl separation buffer. A MACS® LS separation column (Miltenyi Biotec, Bergisch Gladbach, Germany) was placed in the QuadroMACS™ separation unit (Miltenyi Biotec, Bergisch Gladbach, Germany) and washed with 3 ml separation buffer. The cell suspension was applied to the column and the column was washed three times with 3 ml separation buffer. The column was then removed from the magnetic field and B-cells were flushed out with 5 ml separation buffer into a clean falcon tube. Cells were collected by centrifugation at 200 g for 5 min at room temperature, resuspended in culture media and seeded at a cell density of 0.5 x 10^6 cells/ml.

Transient transfection, stable transfection and siRNA interference. Transient and stable transfections were carried out using the lipofectamine™ 2000 transfection reagent (Invitrogen Inc., Carlsbad, CA) based on the manufacturer's recommendations. The quantity of DNA transfected is indicated in each experiment. In the construction of the p21 stable cell lines, HCT116 $p21^{-/-}$ cells were transfected with pIRESpuro2 vector (Clontech, CA) expressing full length p21 and puromycin-N-acetyl-transferase. After 24 hr incubation at 37°C, cells containing the plasmid were selected for by the addition of puromycin (Calbiochem, Nottingham, UK). Fresh medium containing 5 μg/ml puromycin was added after a majority of cells died. Individual colonies were selected and expanded under selection conditions. Small interfering RNA (siRNA) mediated gene knock-down was achieved by transfecting siRNAs (Dharmacon Inc., IL) into cells using Lipofectamine™ 2000 (Invitrogen Inc., Carlsbad, CA) in accordance with the manufacturer's recommendations. p21 siRNA, MDM2 siRNA and control siRNA (*SMART*pool™ Dharmacon Inc., IL) were used at a final concentration of 33 nM. After transfection cells were incubated at 37°C in 5% CO_2 for 24–48 hr, harvested and analyzed by immunoblotting.

Genotoxic or drug treatments of cells. Cells were grown to 70% confluency before treating with indicated drug or stress. Cells were irradiated in culture medium using a Faxitron® cabinet X-ray system, 43855D (Faxitron X-ray Corporation, Lincolnshire, IL USA), at a central dose rate of 2 Gy/min. Cells were irradiated at the stated doses and harvested at the stated time points. Cells were treated with various small molecule inhibitors including Nutlin-3 (Sigma, Dorset, UK), KU55933 and NU7441 (a kind gift from KuDOS Pharmaceuticals, Cambridge, UK). Cyclohexamide was dissolved in DMSO at a stock concentration of 100 mg/ml and added directly into the culture media at a final concentration of 30 μg/ml. Cells were harvested at 0 hr, 0.5 hr, 1 hr, 2 hr, 4 hr after treatment and analyzed by immunoblotting. Polyinosinic polycytidylic acid [poly(I).poly(C)] (Sigma) was dissolved in 0.5 M Hepes pH 7.5 at a stock concentration of 25 mg/ml. The stated concentration was added to cells in culture medium, and cells were harvested at the stated time points.

Protein detection. Cells were lysed in urea lysis buffer (7 M urea, 0.1 M DTT, 0.05% Triton X-100, 25 mM NaCl, 20 mM Hepes pH 7.5). Equal amounts of protein were separated by SDS polyacrylamide gel electrophoresis (SDS PAGE), transferred to Hybond-C nitrocellulose membrane (Amersham Pharmacia Biotech, Buckinghamshire, UK) and hybridized to an appropriate primary antibody and HRP-conjugated secondary antibody for subsequent detection by ECL. Following SDS-PAGE, resolved proteins were Coommassie stained. Protein staining of polyacrylamide gels was achieved by a 30 min incubation with Coommassie blue solution (45% Methanol, 10% Acetic acid, 0.1% w/v Coomassie Blue R250). Gels were destained by incubating with destain (5% (v/v) Methanol, 7% (v/v) Acetic

acid) until bands became visible and background staining was removed.

p53 gene reporter assay. Cells were seeded into 6-well plates, and incubated until ~70% confluency was obtained before being transfected with 1 μg pGL3p21-Luc and 1 μg pCMVβ-Gal DNA. Cells were incubated for 24 hr at 37°C. Cells were then treated and lysed at stated time points. To lyse, cells were washed twice in ice-cold PBS and lysed in 70 μl 5x Reporter Lysis Buffer (Promega, Madison, WI) on ice for 10 min. The cells were scraped and spun at 15,000 g for 2 min at 4°C. The supernatant was transferred to a fresh microcentrifuge tube and snap frozen in liquid nitrogen. For the Luciferase assay, the lysates (20 μl) were aliquoted into a white Microlite2™ 96-well ELISA plate (CoStar; Corning Inc., CA) on ice. 50 μl of Luciferase Substrate™ from the Luciferase Assay Systems™ (Promega, Madison, WI) kit was added to each well of the Microlite2 plate, and allowed to reach room temperature. Luciferase activity was quantified using a luminometer (Fluroskan Ascent FL, Thermo Fisher Scientific, MA). For the β-Galactosidase assay, the lysates (20 μl) were aliquoted into a clear 96-well plate at room temperature, and 20 μl of β-Galactosidase 2x assay buffer (Promega, Madison, WI) was added and incubated for 20 min at 37°C. β-Galactosidase activity was quantified using a PowerwaveXS™ Microplate Spectrophotometer (Bio-Tek, VT) at a wavelength of 405 nm. The results were normalized to account for variation in transfection efficiency, by dividing the Luciferase readout by the β-galactosidase readout to give relative light units.

Proteasome activity assay. Active proteasomes were obtained from cells as described in reference 66. Harvested cells were lysed with proteasome lysis buffer (20 mM Tris-HCl pH 7.2, 0.1 mM EDTA, 1 mM 2-mercaptoethanol, 5 mM ATP, 20% glycerol and 0.04% NP40) by repeated pipetting, followed by a 20 min incubation on ice. Cell lysates were centrifuged at 16,000 g at 4°C for 10 min. Proteasome activity was analyzed using a 20S Proteasome Assay Kit (Calbiochem®, Darmstadt, Germany) in accordance with the manufacturer's recommendations. The 20S activity is measured by monitoring the release of free AMC (7-amino 4-methylcoumarin) from the fluorogenic proteasome specific peptide Suc-Leu-Leu-Val-Tyr-AMC. The rate of AMC release is measured by fluorescence spectroscopy. Cell lysates (final concentration 0.02 mg/ml) were diluted in 190 μl SDS activated Reaction Buffer, added to a white Microlite2™ 96-well ELISA plate (CoStar; Corning Inc., CA) and equilibrated to 37°C. The reaction was initiated by adding 10 μl of the fluorogenic peptide solution to each well. The intensity of fluorescence of each reaction was measured over time by fluorescence spectroscopy (excitation max: ~380 nm; emission max: ~460 nm) using an Envision fluorescence detector (Perkin Elmer, MA).

Subcellular proteome extraction. The ProteoExtract® Subcellular Proteome Extraction Kit (Calbiochem®, Darmstadt, Germany), here after referred to as S-PEK, was used to extract proteins from mammalian cells according to their subcellular localization. The kit was used in accordance with the manufacturer's recommendations. All extraction buffers contain protease inhibitors and all steps were carried out at 4°C unless stated. All fractions were stored at -70°C and analyzed by immunoblotting.

Chromatin protein preparation: Cell fractionation and nuclease digestion. Cells were fractionated by the method of Gilbert and Allan.[42] 5 x 10^6 cells were seeded in 15 cm diameter culture dishes and grown until 80% confluent. Cells were trypsinized and the cell pellet resuspended in 5 ml NBA (85 mM KCl, 5.5% (w/v) sucrose, 10 mM Tris-HCl pH 7.5, 0.2 mM EDTA, 0.5 mM spermidine, 250 μM PMSF). An equal amount of NBB (85 mM KCl, 5.5% (w/v) sucrose, 10 mM Tris-HCl pH 7.5, 0.2 mM EDTA, 0.5 mM spermidine, 250 μM PMSF, 0.1% (v/v) NP40) was added and the cells were incubated on ice for 3 min. A sample was taken of total cellular extract, mixed with an equal volume of SDS sample buffer and stored at -20°C. The nuclei were pelleted by centrifugation at 360 g for 4 min at 4°C. Nuclei were resuspended in NBR (85 mM KCl, 5.5% (w/v) sucrose, 10 mM Tris-HCl pH 7.5, 1.5 mM $CaCl_2$, 3 mM $MgCl_2$, 250 μM PMSF) and digested with 8–14 units of micrococcal nuclease (Worthington) per 20 A_{260} units of nuclei for 10 min on ice in the presence of 100 μg/ml RNaseA. The reaction was stopped by adding 10 mM EDTA. The nuclei were washed, resuspended in $TEEP_{20}$ (10 mM Tris-HCl pH 8.0, 1 mM EDTA, 1 mM EGTA, 250 μM PMSF, 20 mM NaCl) and incubated at 4°C overnight. Nuclear debris was removed leaving soluble chromatin in the supernatant by centrifugation at 12,000 g for 5 min at 4°C. A sample of both the insoluble nuclear fraction and the soluble chromatin containing fraction was removed, mixed with an equal amount of SDS sample buffer and stored at -20°C. All fractions were resolved by SDS-PAGE and analyzed by immunoblotting.

DNA microarray. The Oligo GEArray® p53 Signaling Pathway Microarray for human and mouse was used to profile the expression of 113 genes related to p53 mediated signal transduction (SuperArray, SABiosciences, Fredrick, MD). The system was used according to the manufacturer's instructions. Total RNA was isolated from cells using the RNeasy kit (Qiagen) according to the manufacturer's instructions. TrueLabeling-AMP™ 2.0 (SuperArray) is designed to amplify and label antisense RNA for hybridization to Oligo GEArray® and was used according to the manufacturer's instructions. cDNA was synthesized from total RNA, and used as the template for cRNA synthesis in the presence of biotinylated-UTP, leading to the incorporating biotin labelled uridine into the newly synthesized cRNA. The cRNA was purified using the SuperArray ArrayGrade™ cRNA cleanup kit, according to the manufacturer's instructions. The cRNA was hybridized to the array following the Oligo GEArray® HybTube Protocol. The array membrane was pre-wet with deionized water. GEAhyb Hybridization Solution (SuperArray) was warmed to 60°C, added to the membrane and incubated for 2 hr at 60°C in a hybridization oven with slow agitation. 3 μg biotin labelled cRNA target was mixed with GEAhyb Hybridization Solution, added to the membrane, and allowed to hybridize overnight at 60°C with slow rotation. The membrane was repeatedly washed, then cooled to room temperature. To prevent non-specific binding, the membrane was blocked with GEAblocking Solution Q (SuperArray) for 40 min with continuous rotation at room temperature. The blocking solution was discarded and membrane

was incubated with alkaline phosphatase-conjugated streptavidin. The membrane was repeatedly washed, before being incubated with CDP-Star chemiluminescent substrate (SuperArray). Excess CDP-Star solution was removed from the membrane and array image was acquired by exposure to X-ray film (Kodak, NY). The resulting images were scanned and saved as 16 bit TIFF files. The images were uploaded into the GEArray Expression Analysis Suite program (geasuite.superarray.com) which was used to convert the fluorescent intensity of the probe into values representing gene expression, and allow data analysis and quantitation of the microarray results.

Acknowledgements

L.Y.P. was supported by a BBSRC Ph.D., studentship and T.R.H. lab is supported in part by a CR-UK Programme Grant C483/A6354.

References

1. Dey A, Lane DP, Verma CS. Modulating the p53 pathway. Semin Cancer Biol 2010; 20:3-9.
2. Vousden KH, Lane DP. p53 in health and disease. Nat Rev Mol Cell Biol 2007; 8:275-83.
3. MacLaine NJ, Hupp TR. The regulation of p53 by phosphorylation: A model for how distinct signals integrate into the p53 pathway. Aging 2009; 1:490-502.
4. Bartek J, Lukas J. Chk1 and Chk2 kinases in checkpoint control and cancer. Cancer Cell 2003; 3:421-9.
5. Hupp TR, Walkinshaw M. Multienzyme assembly of a p53 transcription complex. Nat Struct Mol Biol 2007; 14:885-7.
6. Carter S, Bischof O, Dejean A, Vousden KH. C-terminal modifications regulate MDM2 dissociation and nuclear export of p53. Nat Cell Biol 2007; 9:428-35.
7. Michael D, Oren M. The p53-Mdm2 module and the ubiquitin system. Semin Cancer Biol 2003; 13:49-58.
8. Ma L, Wagner J, Rice JJ, Hu W, Levine AJ, Stolovitzky GA. A plausible model for the digital response of p53 to DNA damage. Proc Natl Acad Sci USA 2005; 102:14266-71.
9. Wagner J, Ma L, Rice JJ, Hu W, Levine AJ, Stolovitzky GA. p53-Mdm2 loop controlled by a balance of its feedback strength and effective dampening using ATM and delayed feedback. Syst Biol (Stevenage) 2005; 152:109-18.
10. Lu X, Ma O, Nguyen TA, Jones SN, Oren M, Donehower LA. The Wip1 Phosphatase acts as a gatekeeper in the p53-Mdm2 autoregulatory loop. Cancer Cell 2007; 12:342-54.
11. Maya R, Balass M, Kim ST, Shkedy D, Leal JF, Shifman O, et al. ATM-dependent phosphorylation of Mdm2 on serine 395: Role in p53 activation by DNA damage. Genes Dev 2001; 15:1067-77.
12. Batchelor E, Mock CS, Bhan I, Loewer A, Lahav G. Recurrent initiation: A mechanism for triggering p53 pulses in response to DNA damage. Mol Cell 2008; 30:277-89.
13. Johnson TM, Attardi LD. Dissecting p53 tumor suppressor function in vivo through the analysis of genetically modified mice. Cell Death Differ 2006; 13:902-8.
14. Donehower LA, Harvey M, Slagle BL, McArthur MJ, Montgomery CA Jr, Butel JS, et al. Mice deficient for p53 are developmentally normal but susceptible to spontaneous tumours. Nature 1992; 356:215-21.
15. Garcia-Cao I, Garcia-Cao M, Martin-Caballero J, Criado LM, Klatt P, Flores JM, et al. "Super p53" mice exhibit enhanced DNA damage response, are tumor resistant and age normally. EMBO J 2002; 21:6225-35.
16. Kemp CJ, Donehower LA, Bradley A, Balmain A. Reduction of p53 gene dosage does not increase initiation or promotion but enhances malignant progression of chemically induced skin tumors. Cell 1993; 74:813-22.
17. Lowe SW, Ruley HE, Jacks T, Housman DE. p53-dependent apoptosis modulates the cytotoxicity of anticancer agents. Cell 1993; 74:957-67.
18. Mendrysa SM, O'Leary KA, McElwee MK, Michalowski J, Eisenman RN, Powell DA, et al. Tumor suppression and normal aging in mice with constitutively high p53 activity. Genes Dev 2006; 20:16-21.
19. Lahav G, Rosenfeld N, Sigal A, Geva-Zatorsky N, Levine AJ, Elowitz MB, et al. Dynamics of the p53-Mdm2 feedback loop in individual cells. Nat Genet 2004; 36:147-50.
20. Lev Bar-Or R, Maya R, Segel LA, Alon U, Levine AJ, Oren M. Generation of oscillations by the p53-Mdm2 feedback loop: A theoretical and experimental study. Proc Natl Acad Sci USA 2000; 97:11250-5.
21. Ciliberto A, Novak B, Tyson JJ. Steady states and oscillations in the p53/Mdm2 network. Cell Cycle 2005; 4:488-93.
22. Martin-Caballero J, Flores JM, Garcia-Palencia P, Serrano M. Tumor susceptibility of p21(Waf1/Cip1)-deficient mice. Cancer Res 2001; 61:6234-8.
23. Jackson RJ, Engelman RW, Coppola D, Cantor AB, Wharton W, Pledger WJ. $p21^{Cip1}$ nullizygosity increases tumor metastasis in irradiated mice. Cancer Res 2003; 63:3021-5.
24. Shen KC, Heng H, Wang Y, Lu S, Liu G, Deng CX, et al. ATM and p21 cooperate to suppress aneuploidy and subsequent tumor development. Cancer Res 2005; 65:8747-53.
25. Waldman T, Kinzler KW, Vogelstein B. p21 is necessary for the p53-mediated G_1 arrest in human cancer cells. Cancer Res 1995; 55:5187-90.
26. Broude EV, Demidenko ZN, Vivo C, Swift ME, Davis BM, Blagosklonny MV, et al. p21 (CDKN1A) is a negative regulator of p53 stability. Cell Cycle 2007; 6:1468-71.
27. Muller P, Hrstka R, Coomber D, Lane DP, Vojtesek B. Chaperone-dependent stabilization and degradation of p53 mutants. Oncogene 2008; 27:3371-83.
28. Maki CG, Howley PM. Ubiquitination of p53 and p21 is differentially affected by ionizing and UV radiation. Mol Cell Biol 1997; 17:355-63.
29. Takaoka A, Hayakawa S, Yanai H, Stoiber D, Negishi H, Kikuchi H, et al. Integration of interferon-alpha/beta signalling to p53 responses in tumour suppression and antiviral defence. Nature 2003; 424:516-23.
30. Taura M, Eguma A, Suico MA, Shuto T, Koga T, Komatsu K, et al. p53 regulates Toll-like receptor 3 expression and function in human epithelial cell lines. Mol Cell Biol 2008; 28:6557-67.
31. Bunz F, Hwang PM, Torrance C, Waldman T, Zhang Y, Dillehay L, et al. Disruption of p53 in human cancer cells alters the responses to therapeutic agents. J Clin Invest 1999; 104:263-9.
32. Hayward RL, Macpherson JS, Cummings J, Monia BP, Smyth JF, Jodrell DI. Antisense Bcl-x_l downregulation switches the response to topoisomerase I inhibition from senescence to apoptosis in colorectal cancer cells, enhancing global cytotoxicity. Clin Cancer Res 2003; 9:2856-65.
33. Spierings DC, de Vries EG, Stel AJ, te Rietstap N, Vellenga E, de Jong S. Low $p21^{Waf1/Cip1}$ protein level sensitizes testicular germ cell tumor cells to Fas-mediated apoptosis. Oncogene 2004; 23:4862-72.
34. Dotto GP. p21(WAF1/Cip1): More than a break to the cell cycle? Biochim Biophys Acta 2000; 1471:43-56.
35. Kastan MB, Lim DS, Kim ST, Yang D. ATM: A key determinant of multiple cellular responses to irradiation. Acta Oncol 2001; 40:686-8.
36. Arva NC, Gopen TR, Talbott KE, Campbell LE, Chicas A, White DE, et al. A chromatin-associated and transcriptionally inactive p53-Mdm2 complex occurs in mdm2 SNP309 homozygous cells. J Biol Chem 2005; 280:26776-87.
37. Lain S, Hollick JJ, Campbell J, Staples OD, Higgins M, Aoubala M, et al. Discovery, in vivo activity and mechanism of action of a small-molecule p53 activator. Cancer Cell 2008; 13:454-63.
38. Sepehrnia B, Paz IB, Dasgupta G, Momand J. Heat shock protein 84 forms a complex with mutant p53 protein predominantly within a cytoplasmic compartment of the cell. J Biol Chem 1996; 271:15084-90.
39. Foo RS, Nam YJ, Ostreicher MJ, Metzl MD, Whelan RS, Peng CF, et al. Regulation of p53 tetramerization and nuclear export by ARC. Proc Natl Acad Sci USA 2007; 104:20826-31.
40. Shimizu H, Saliba D, Wallace M, Finlan L, Langridge-Smith PR, Hupp TR. Destabilizing missense mutations in the tumour suppressor protein p53 enhance its ubiquitination in vitro and in vivo. Biochem J 2006; 397:355-67.
41. Terzian T, Suh YA, Iwakuma T, Post SM, Neumann M, Lang GA, et al. The inherent instability of mutant p53 is alleviated by Mdm2 or $p16^{INK4a}$ loss. Genes Dev 2008; 22:1337-44.
42. Gilbert N, Allan J. Distinctive higher-order chromatin structure at mammalian centromeres. Proc Natl Acad Sci USA 2001; 98:11949-54.
43. Kontopidis G, Wu SY, Zheleva DI, Taylor P, McInnes C, Lane DP, et al. Structural and biochemical studies of human proliferating cell nuclear antigen complexes provide a rationale for cyclin association and inhibitor design. Proc Natl Acad Sci USA 2005; 102:1871-6.
44. Prabhu NS, Blagosklonny MV, Zeng YX, Wu GS, Waldman T, El-Deiry WS. Suppression of cancer cell growth by adenovirus expressing p21(WAF1/CIP1) deficient in PCNA interaction. Clin Cancer Res 1996; 2:1221-9.
45. MacPherson D, Kim J, Kim T, Rhee BK, Van Oostrom CT, DiTullio RA, et al. Defective apoptosis and B-cell lymphomas in mice with p53 point mutation at Ser 23. EMBO J 2004; 23:3689-99.
46. Jones JM, Cui XS, Medina D, Donehower LA. Heterozygosity of $p21^{WAF1/CIP1}$ enhances tumor cell proliferation and cyclin D1-associated kinase activity in a murine mammary cancer model. Cell Growth Differ 1999; 10:213-22.
47. Efeyan A, Collado M, Velasco-Miguel S, Serrano M. Genetic dissection of the role of $p21^{Cip1/Waf1}$ in p53-mediated tumour suppression. Oncogene 2007; 26:1645-9.
48. Cole AM, Ridgway RA, Derkits SE, Parry L, Barker N, Clevers H, et al. p21 loss blocks senescence following Apc loss and provokes tumourigenesis in the renal but not the intestinal epithelium. EMBO Mol Med 2010; 2:472-86.
49. Vassilev LT, Vu BT, Graves B, Carvajal D, Podlaski F, Filipovic Z, et al. In vivo activation of the p53 pathway by small-molecule antagonists of MDM2. Science 2004; 303:844-8.
50. Hickson I, Zhao Y, Richardson CJ, Green SJ, Martin NM, Orr AI, et al. Identification and characterization of a novel and specific inhibitor of the ataxia-telangiectasia mutated kinase ATM. Cancer Res 2004; 64:9152-9.

51. Levine AJ, Hu W, Feng Z. The p53 pathway: What questions remain to be explored? Cell Death Differ 2006; 13:1027-36.
52. Clarke AR, Purdie CA, Harrison DJ, Morris RG, Bird CC, Hooper ML, et al. Thymocyte apoptosis induced by p53-dependent and independent pathways. Nature 1993; 362:849-52.
53. el-Deiry WS, Tokino T, Velculescu VE, Levy DB, Parsons R, Trent JM, et al. WAF1, a potential mediator of p53 tumor suppression. Cell 1993; 75:817-25.
54. Harper JW, Adami GR, Wei N, Keyomarsi K, Elledge SJ. The p21 Cdk-interacting protein Cip1 is a potent inhibitor of G_1 cyclin-dependent kinases. Cell 1993; 75:805-16.
55. Blagosklonny MV, Demidenko ZN, Fojo T. Inhibition of transcription results in accumulation of Wt p53 followed by delayed outburst of p53-inducible proteins: p53 as a sensor of transcriptional integrity. Cell Cycle 2002; 1:67-74.
56. Giannakakou P, Robey R, Fojo T, Blagosklonny MV. Low concentrations of paclitaxel induce cell type-dependent p53, p21 and G_1/G_2 arrest instead of mitotic arrest: Molecular determinants of paclitaxel-induced cytotoxicity. Oncogene 2001; 20:3806-13.
57. Scott MT, Ingram A, Ball KL. PDK1-dependent activation of atypical PKC leads to degradation of the p21 tumour modifier protein. EMBO J 2002; 21:6771-80.
58. Scott MT, Morrice N, Ball KL. Reversible phosphorylation at the C-terminal regulatory domain of p21(Waf1/Cip1) modulates proliferating cell nuclear antigen binding. J Biol Chem 2000; 275:11529-37.
59. Xu H, Zhang Z, Li M, Zhang R. MDM2 promotes proteasomal degradation of $p21^{Waf1}$ via a conformation change. J Biol Chem 2010; 285:18407-14.
60. Touitou R, Richardson J, Bose S, Nakanishi M, Rivett J, Allday MJ. A degradation signal located in the C-terminus of $p21^{WAF1/CIP1}$ is a binding site for the C8 alpha-subunit of the 20S proteasome. EMBO J 2001; 20:2367-75.
61. Missero C, Di Cunto F, Kiyokawa H, Koff A, Dotto GP. The absence of $p21^{Cip1/WAF1}$ alters keratinocyte growth and differentiation and promotes ras-tumor progression. Genes Dev 1996; 10:3065-75.
62. Deng C, Zhang P, Harper JW, Elledge SJ, Leder P. Mice lacking $p21^{CIP1/WAF1}$ undergo normal development, but are defective in G_1 checkpoint control. Cell 1995; 82:675-84.
63. Weinberg WC, Azzoli CG, Kadiwar N, Yuspa SH. p53 gene dosage modifies growth and malignant progression of keratinocytes expressing the v-rasHa oncogene. Cancer Res 1994; 54:5584-92.
64. Mihara M, Erster S, Zaika A, Petrenko O, Chittenden T, Pancoska P, et al. p53 has a direct apoptogenic role at the mitochondria. Mol Cell 2003; 11:577-90.
65. Iwakuma T, Lozano G. Crippling p53 activities via knock-in mutations in mouse models. Oncogene 2007; 26:2177-84.
66. Araya J, Maruyama M, Inoue A, Fujita T, Kawahara J, Sassa K, et al. Inhibition of proteasome activity is involved in cobalt-induced apoptosis of human alveolar macrophages. Am J Physiol Lung Cell Mol Physiol 2002; 283:849-58.